

**They are not third parties:
solutes and polymers in fluid-structure
interaction**

**Pilhwa Lee
07/11/2016**

**Molecular and Integrative Physiology
University of Michigan**

Cardiac differentiation

Dendritic spine motility

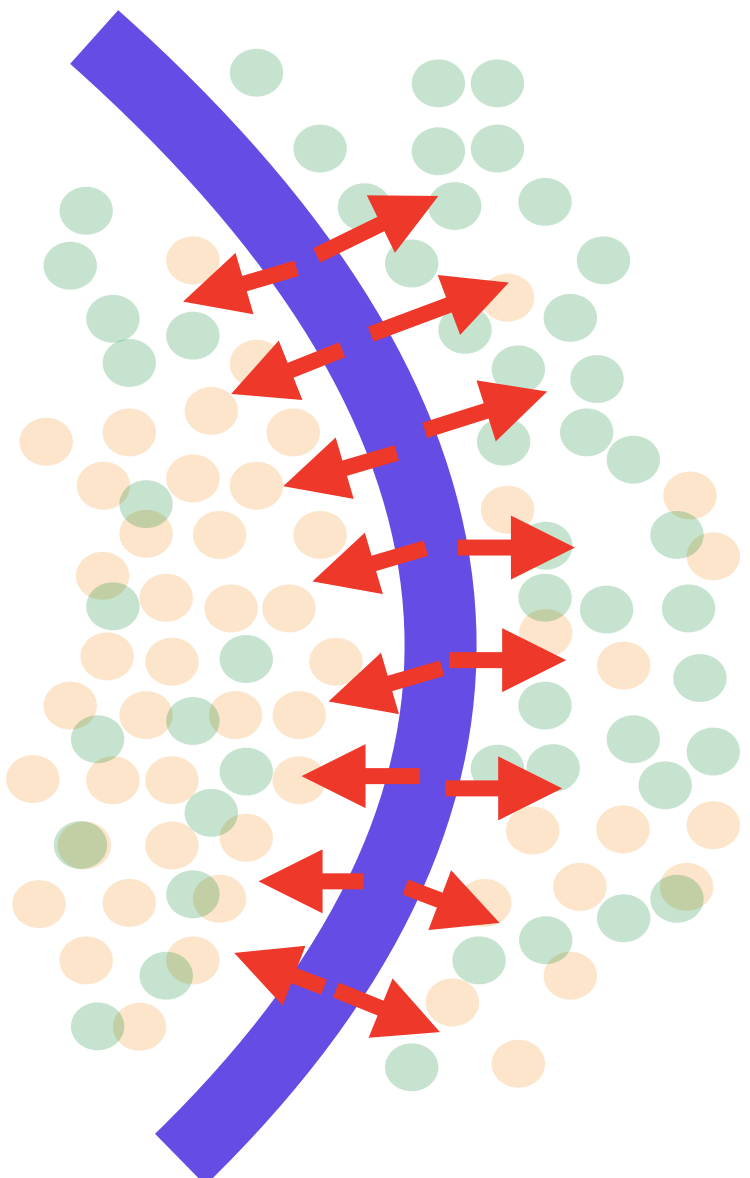
The Immersed Boundary Method

- i) Advection-electrodiffusion
- ii) Two-phase viscoelastic fluids and gels

Renal peristaltic concentration

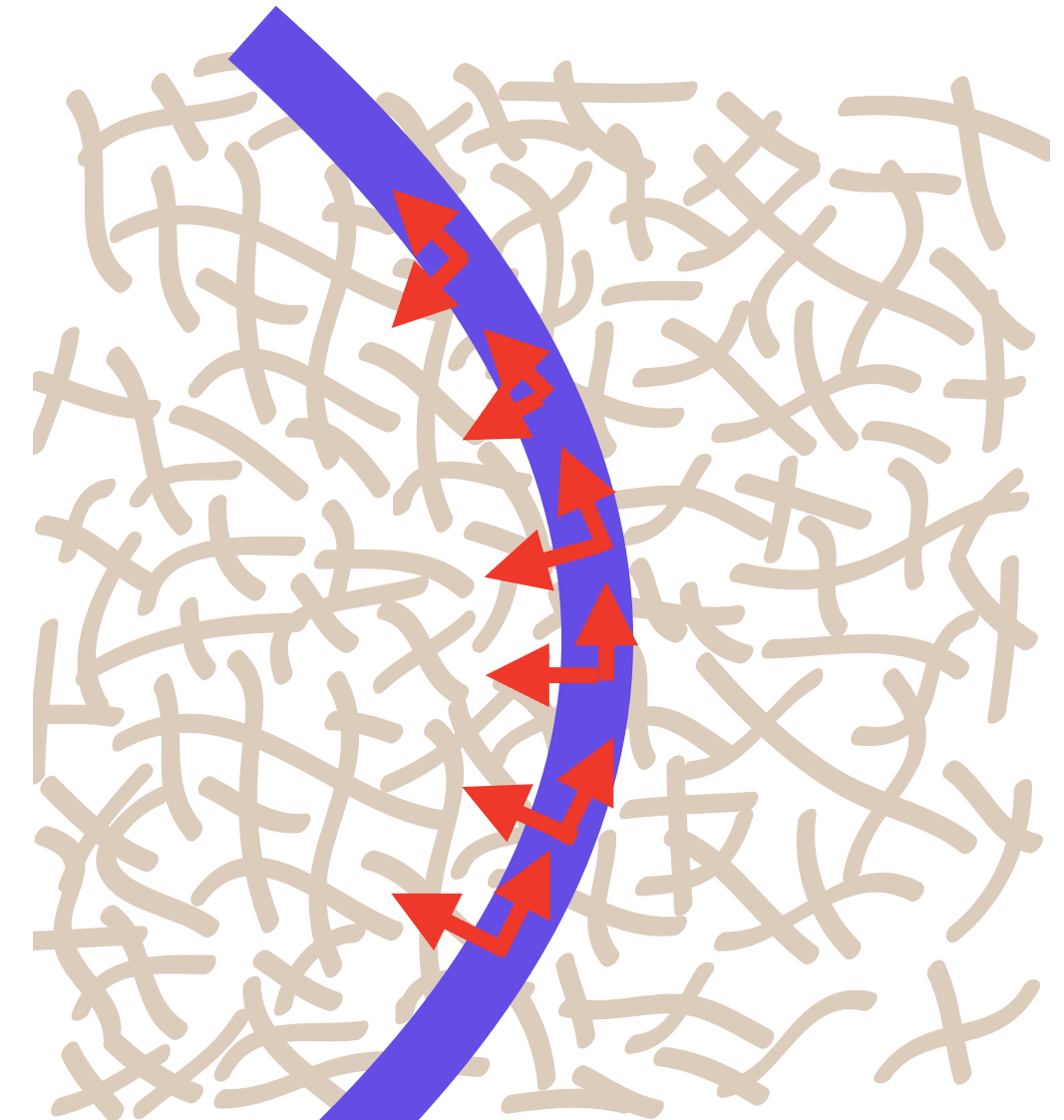
Non-Newtonian swimming

Fluid-structure interaction with solutes/polymers



$$-\frac{\delta E}{\delta \mathbf{X}} = \mathbf{F}_{\text{ms}} + \mathbf{F}_{\text{mf}}$$

Chemical potential barrier



$$-\frac{\delta E}{\delta \mathbf{X}} = \mathbf{F}_{\text{mp}} + \mathbf{F}_{\text{mf}}$$

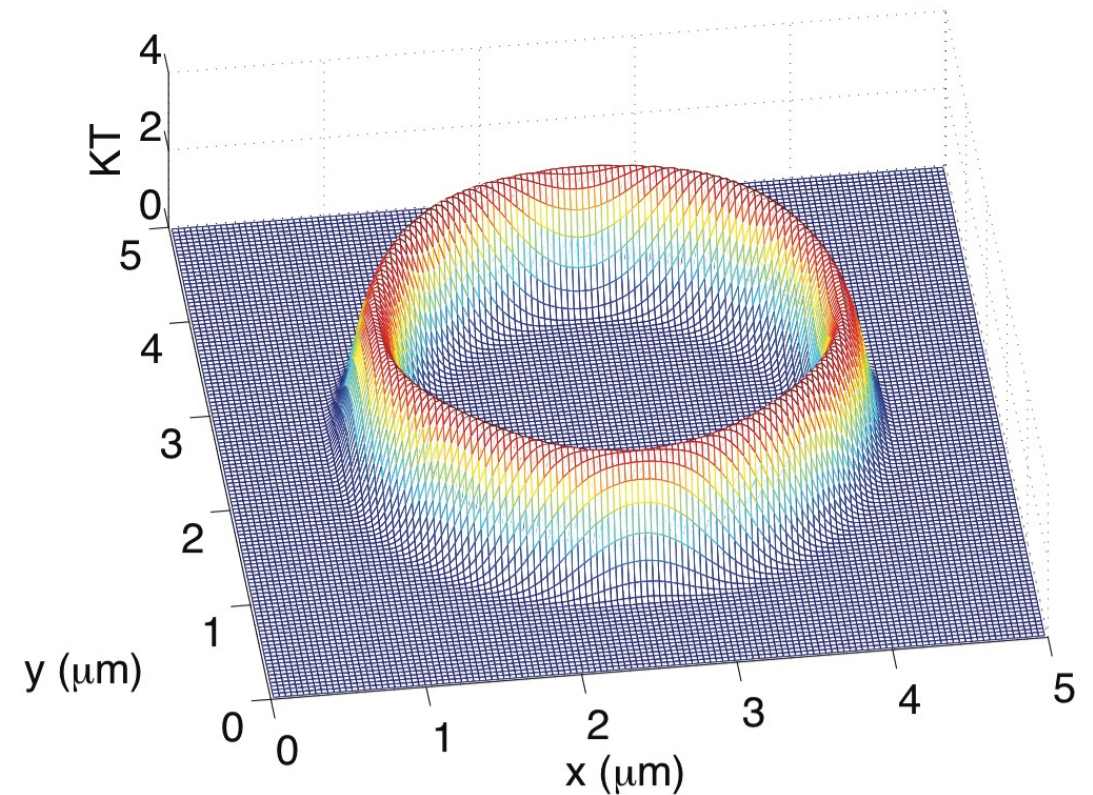
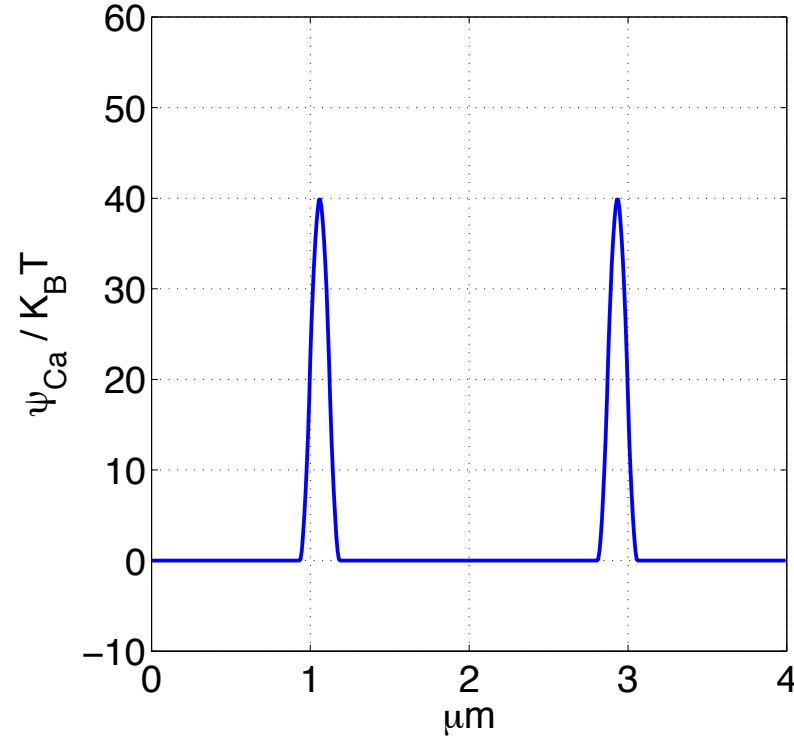
Resistive drag

IB method for advection-electrodiffusion

Chemical potential barrier

$$\psi_i(\mathbf{x}, t) = \int_{\Omega_L} \Psi(\mathbf{x} - \mathbf{X}(s, t)) A_i(s, t) ds$$

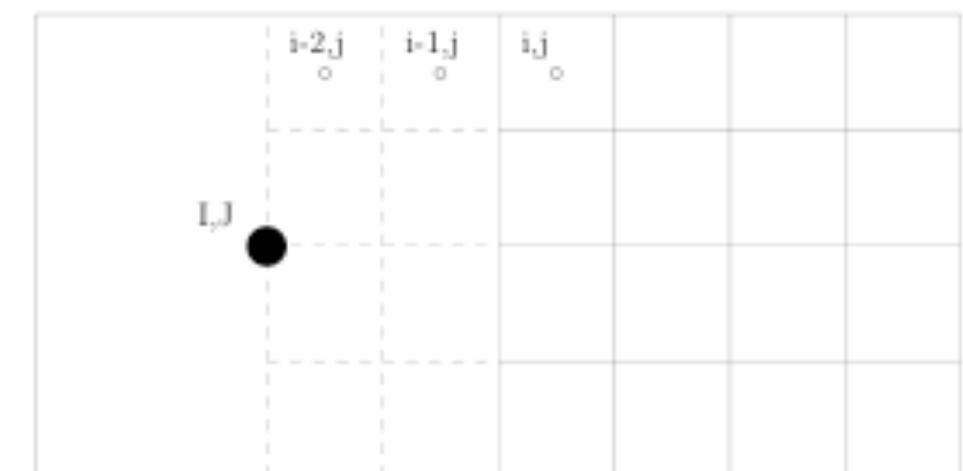
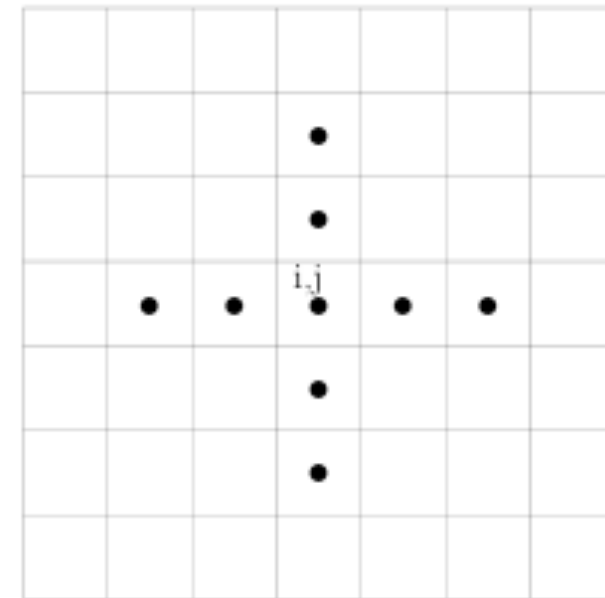
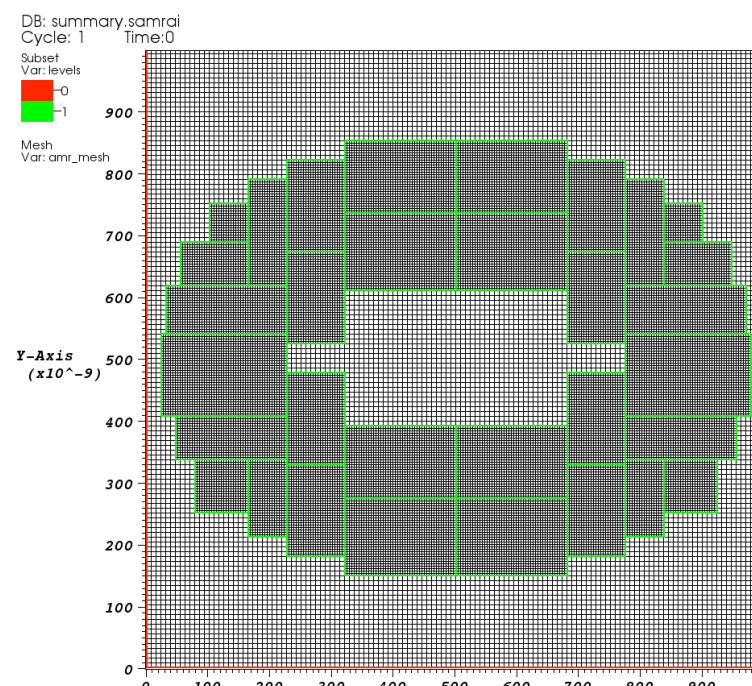
$$\mathbf{F}_{ms}(s, t) = \int_{\Omega_E} \sum_k (-\nabla \Psi(\mathbf{x} - \mathbf{X}(s, t)) A_k(s, t) c_k(\mathbf{x}, t) d\mathbf{x}$$



IB method for advection-electrodiffusion

Fast composite multigrid

- PETSc
- SAMRAI - multilevel adaptive mesh refinement
- Hypre - algebraic multigrid



IB method for advection-electrodiffusion

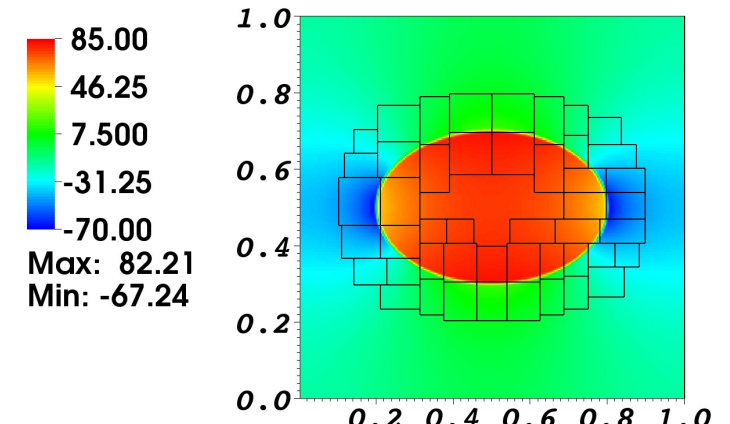
The Stokes equations with permeable membrane

$$\rho \frac{\tilde{\mathbf{u}} - \mathbf{u}^n}{\Delta t} + \mathbf{D}_h p^{n-\frac{1}{2}} = \mu L_h \frac{\tilde{\mathbf{u}} + \mathbf{u}^n}{2} + \mathbf{S}_n \mathbf{F}_{\text{mf}}^{n+1} + \mathbf{f}_b^n$$

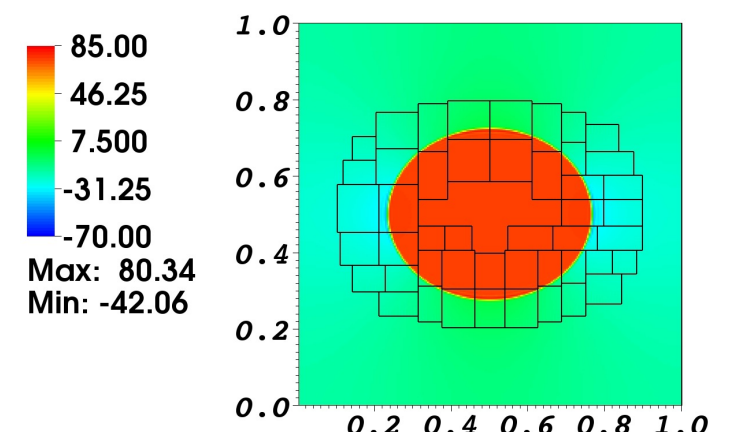
$$\mathbf{u}^{n+1} = P\tilde{\mathbf{u}}$$

$$\zeta \left(\frac{\mathbf{X}^{n+1} - \mathbf{X}^n}{\Delta t} - \frac{\mathbf{U}^{n+1} + \mathbf{U}^n}{2} \right) = (\mathbf{F}_{\text{mf}}^{n+1} \cdot \mathbf{N}_n) \mathbf{N}_n$$

$$p^{n+1/2} = p^{n-1/2} + \left(\frac{\rho}{\Delta t} L^{-1} - \frac{\mu}{2} I \right) \mathbf{D}_h \cdot \tilde{\mathbf{u}}$$



- Fast adaptive composite (FAC) method: preconditioner
- One layer of ghost cells, bottom solver (PFMG)
- Krylov subspace GMRES: main solver
- Cell-centered approximate projection method



IB method for advection-electrodiffusion

$$\frac{c_i^{n+1} - c_i^n}{\Delta t} + \mathbf{D}_h \cdot \mathbf{J}_i^{n+1} = 0$$

$$\mathbf{J}_i^{n+1} = -D_i(D_h c_i^{n+1}) + [\frac{D_i}{K_B T}(-qz_i D_h \varphi^n - D_h \psi_i^n) + \mathbf{u}^n] c_i^{n+1}$$

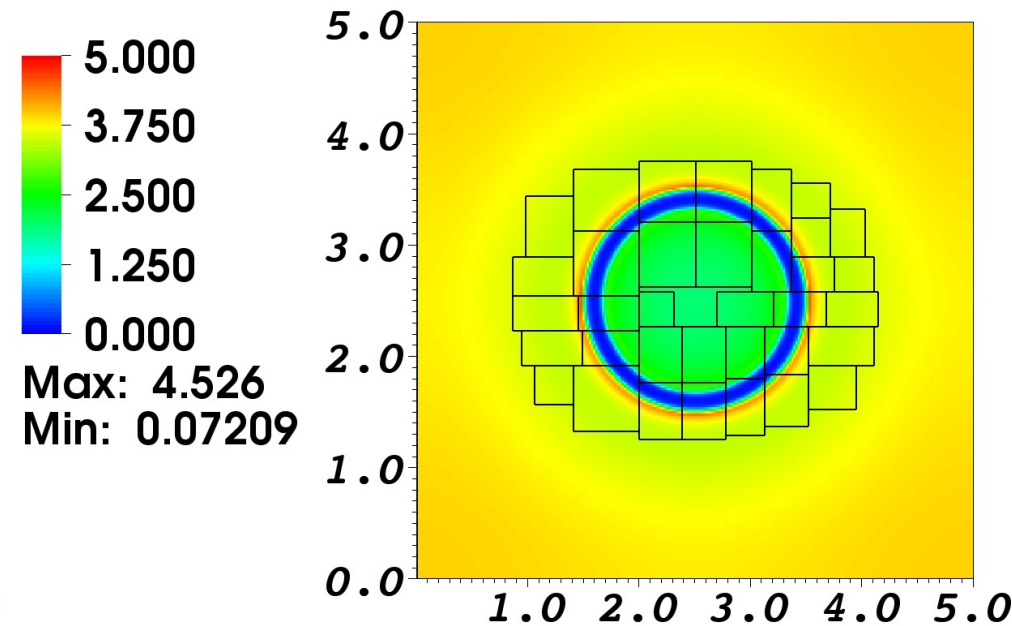
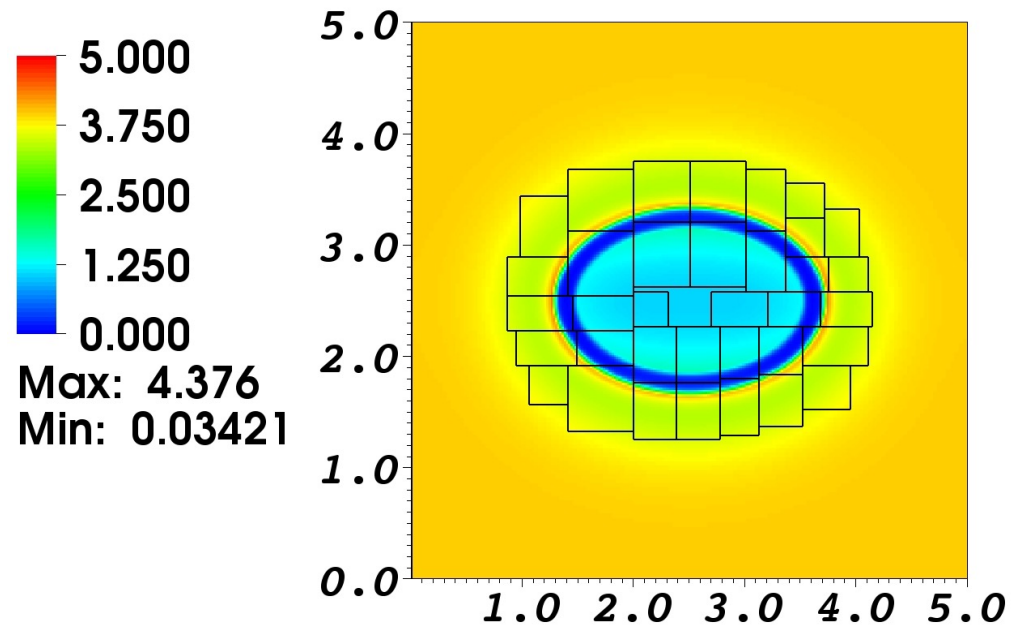
$$-L_h \varphi^n = (\sum_i qz_i^n c_i^n + \rho_b)/\epsilon$$

$$L_i^n c_i^{n+1} = c_i^n$$

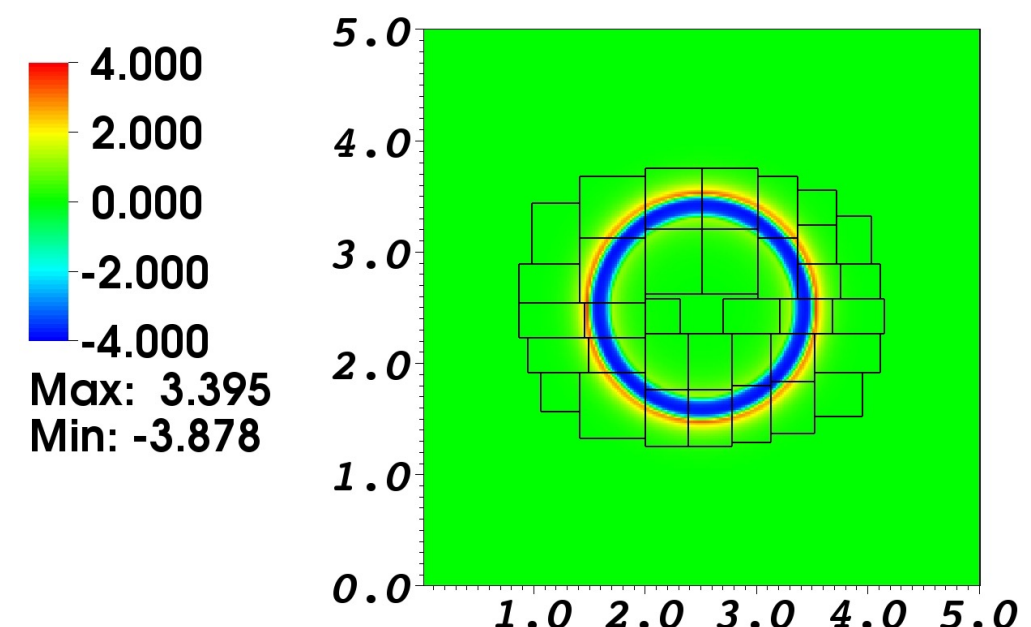
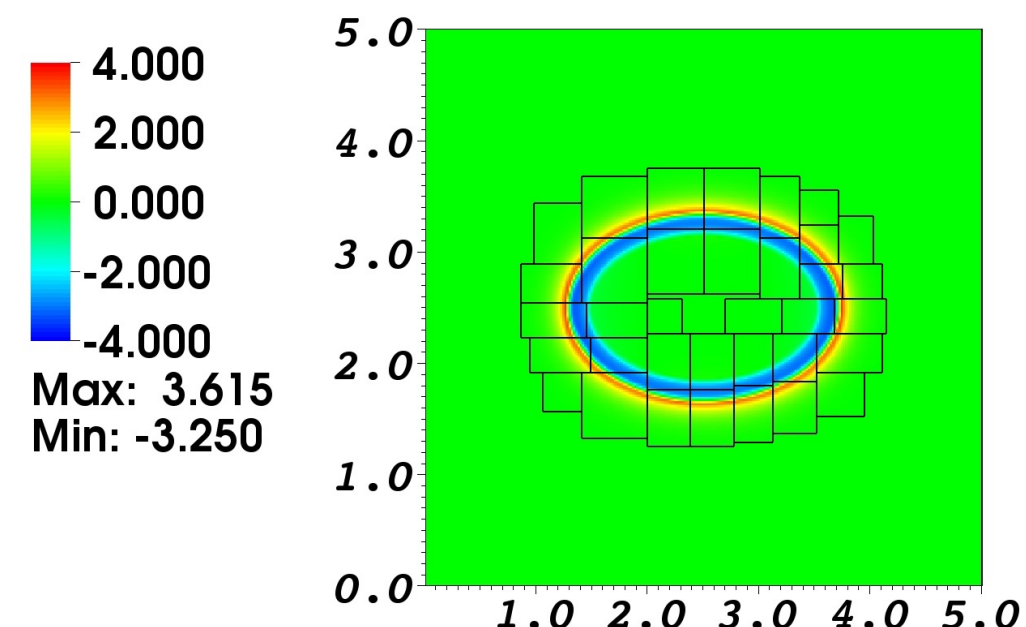
$$L_i^n = L(\mathbf{u}^n, \varphi^n, \psi_i^n)$$

- Fast adaptive composite (FAC) method, preconditioner
- two layers of ghost cells
- bottom solver (PFMG), first order upwind
- GMRES, main solver

IB method for advection-electrodiffusion

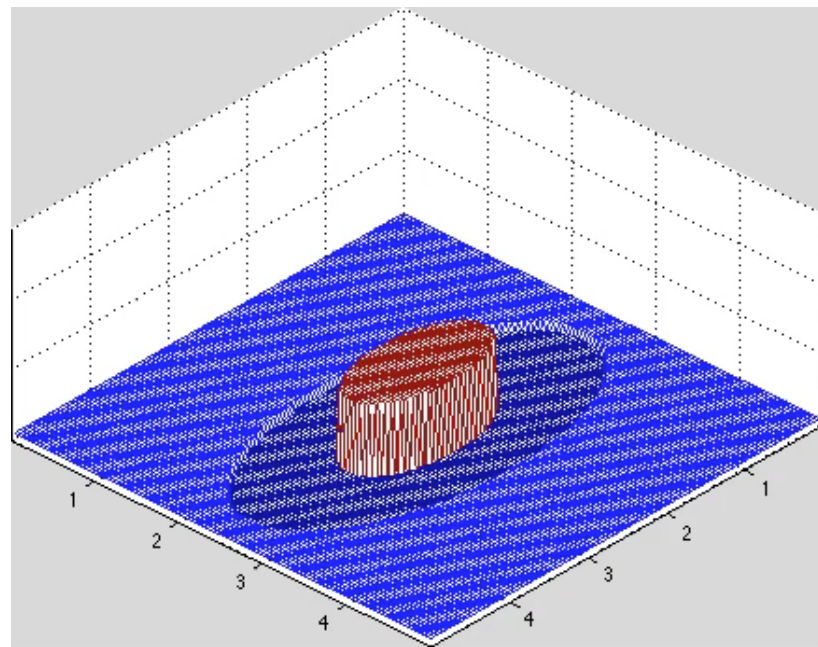


[Ca⁺⁺] distribution

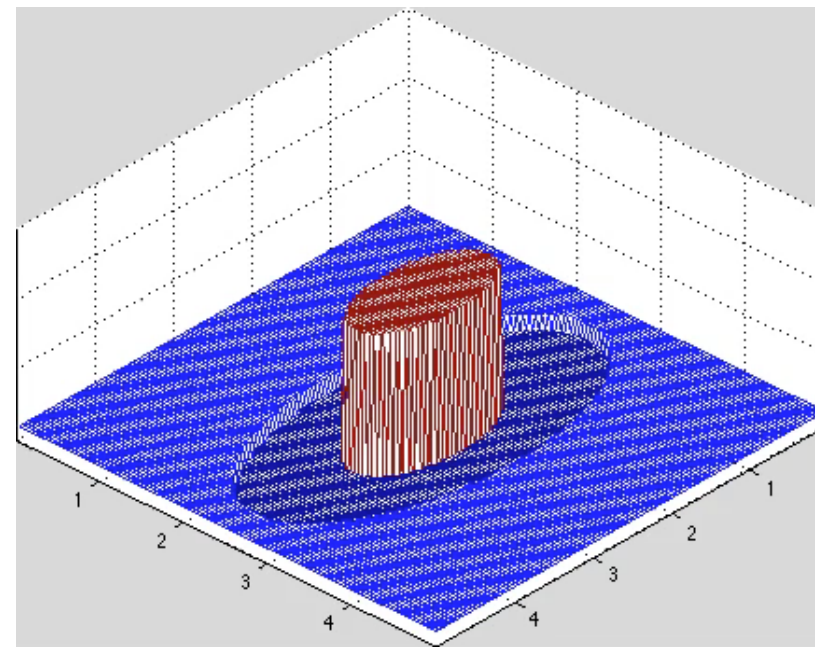


Electrical charge density distribution

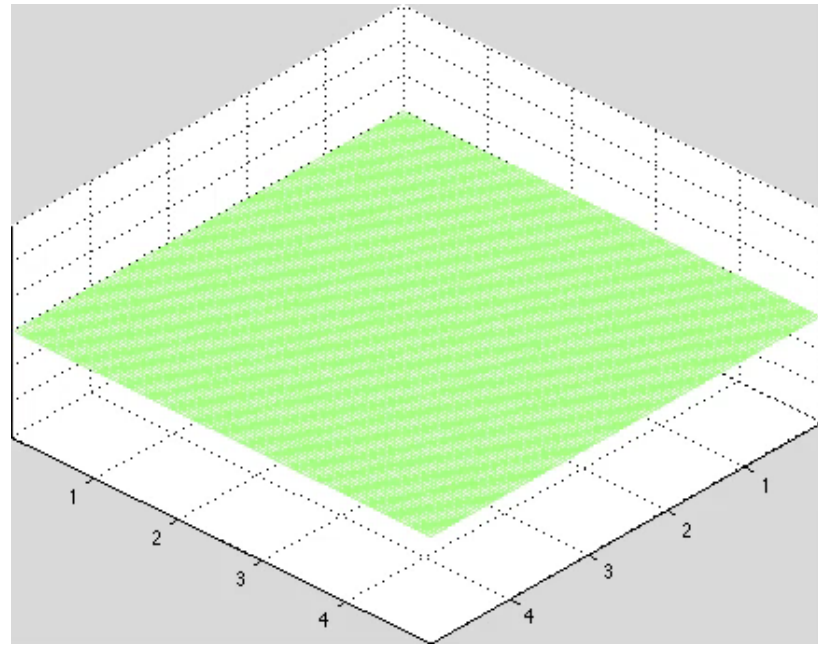
Concentration dependent contraction



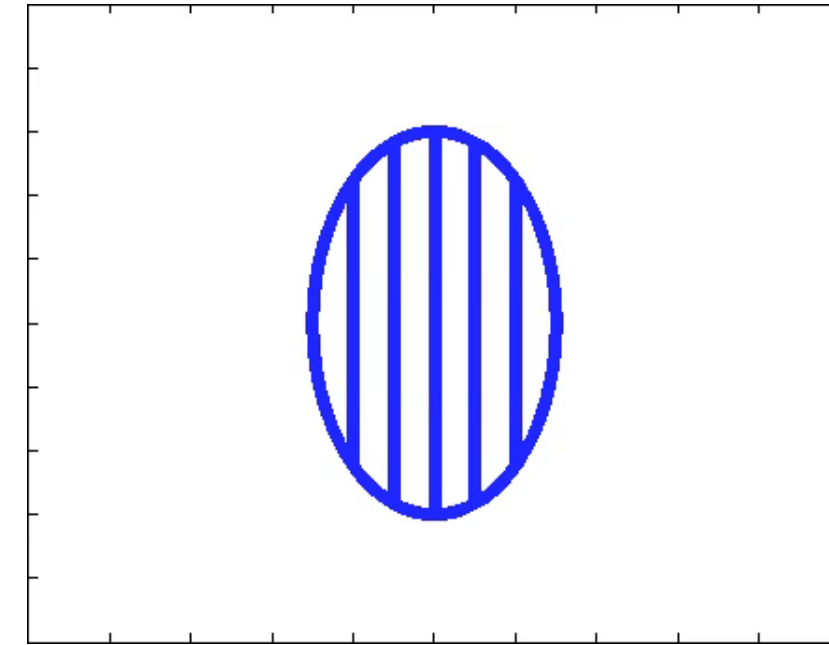
[Ca⁺⁺] spatial distribution



[Cl⁻] spatial distribution

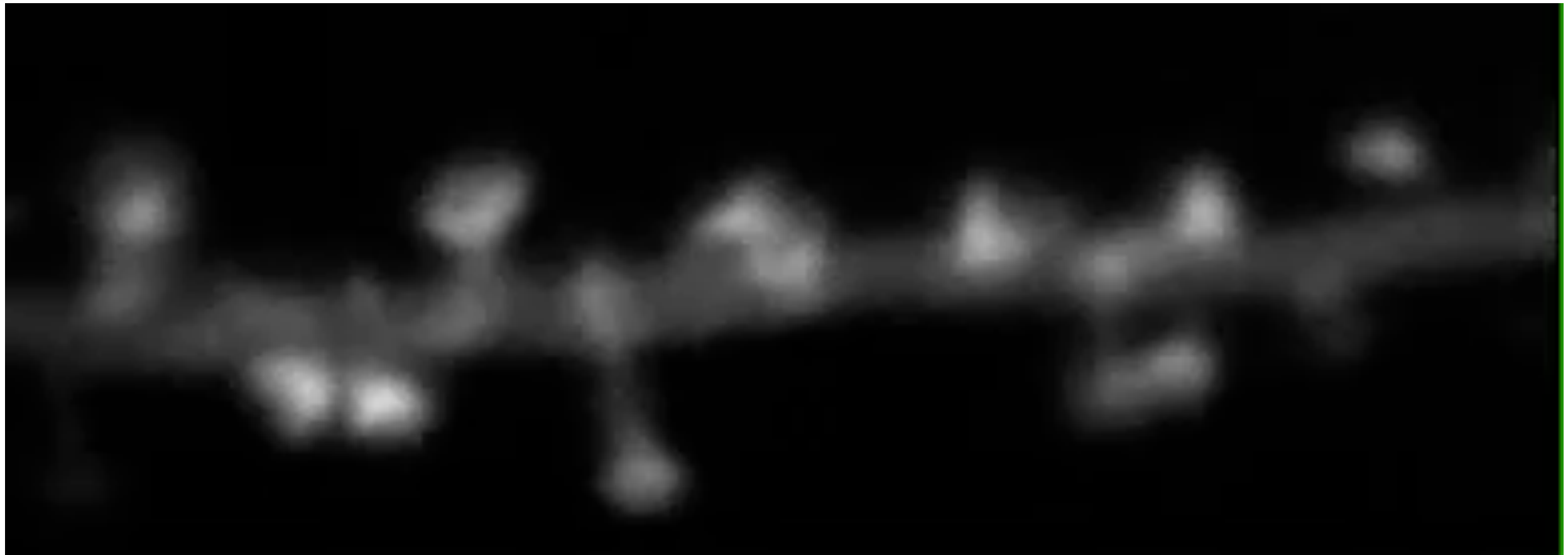


Electrical charge density spatial distribution



Contraction of actomyosin fibers

Dendritic spine motility and dendritic integration

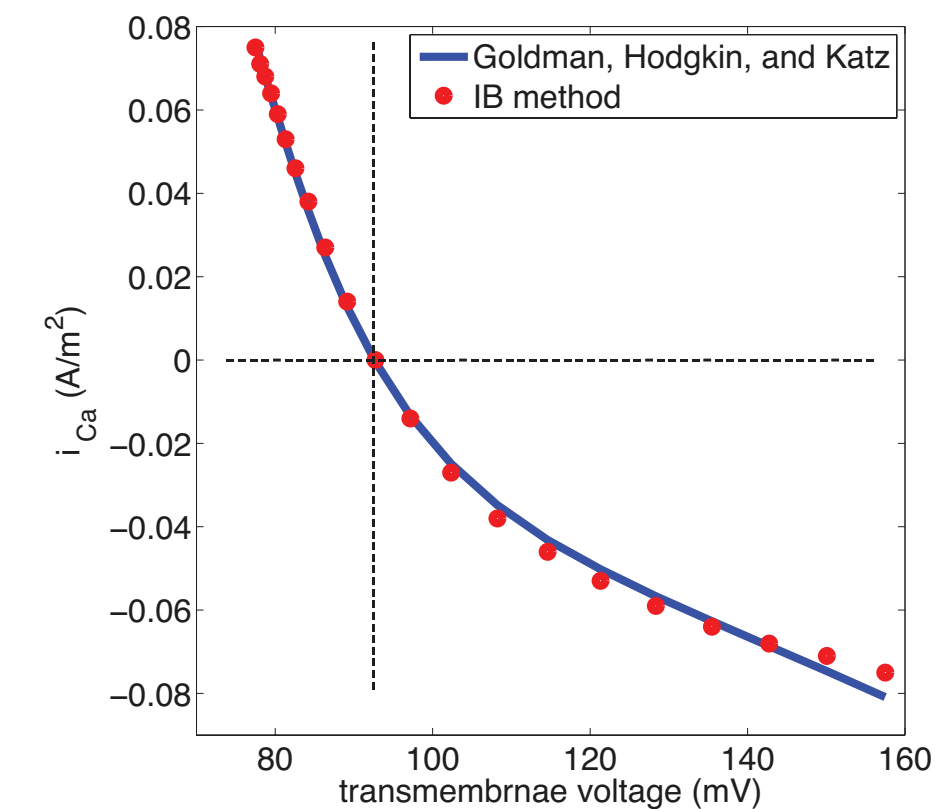
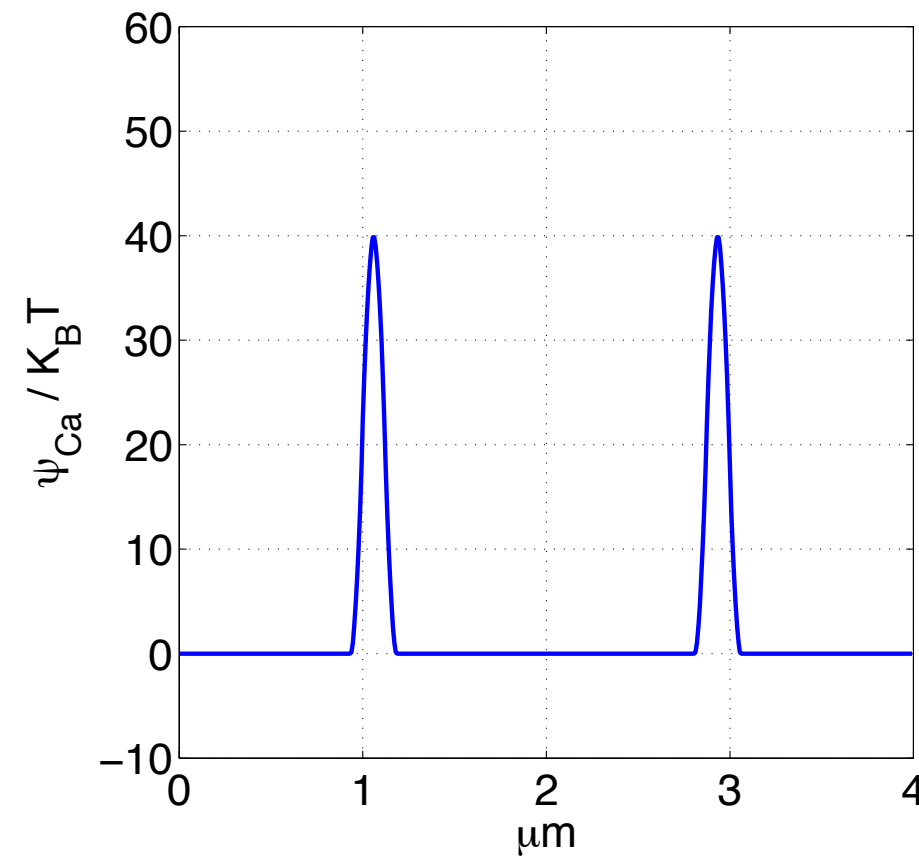


Matus, et al. 2006

How the following signals in dendritic spines change calcium dynamics and structural plasticity in dendrites and functionality in neural circuits?

- Myosin II activation
- Wnt signaling
- Amyloid beta aggregation

Voltage sensitive calcium ion channels in a dendritic spine



Membrane physiology
Interface boundary condition



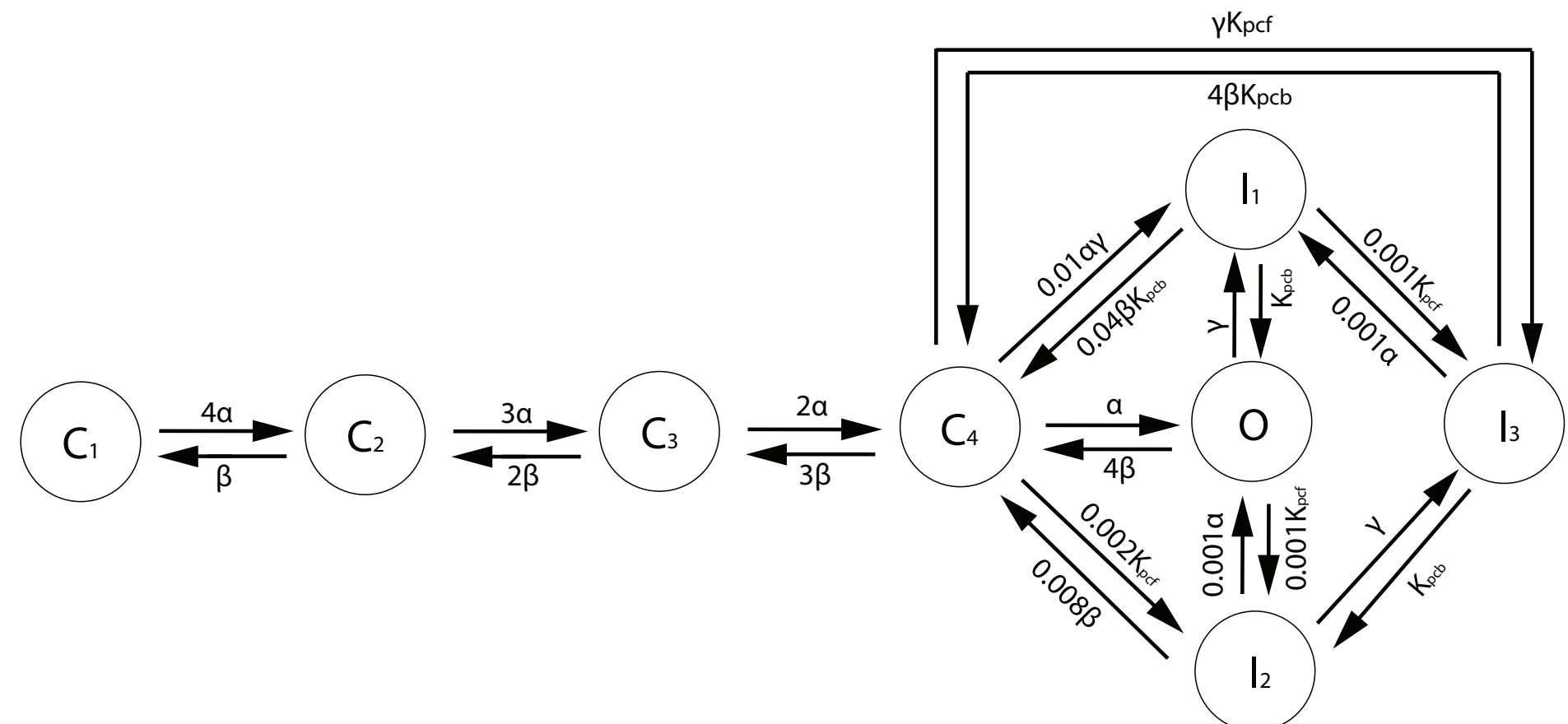
Chemical potential barrier

Voltage sensitive calcium ion channels in a dendritic spine

Continuous-time Markov process

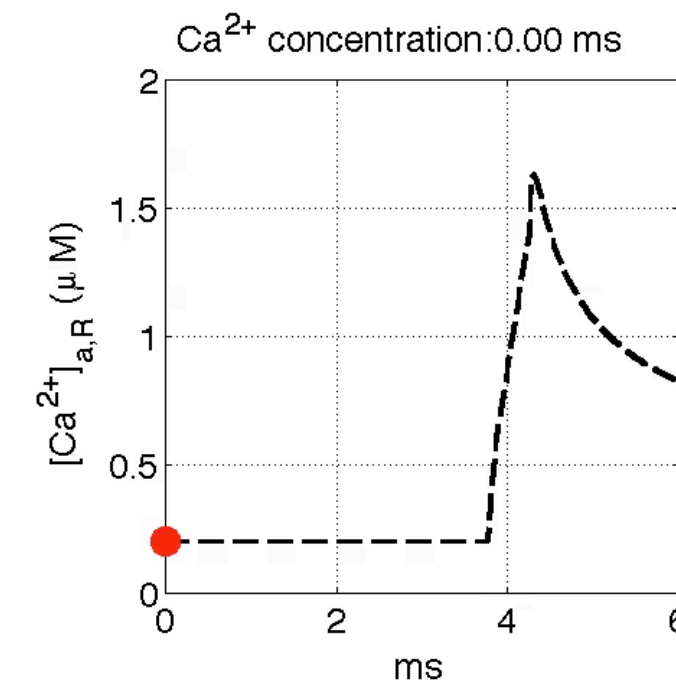
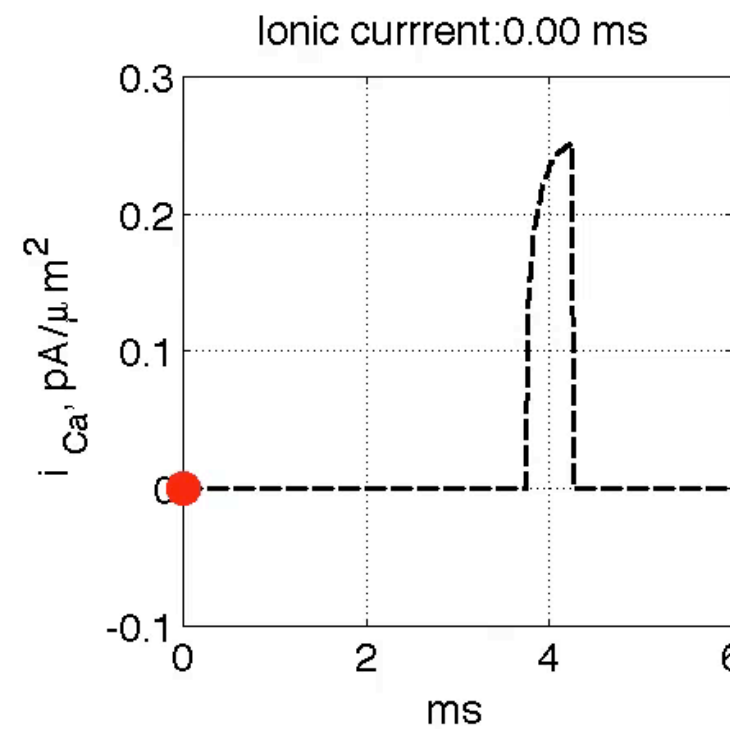
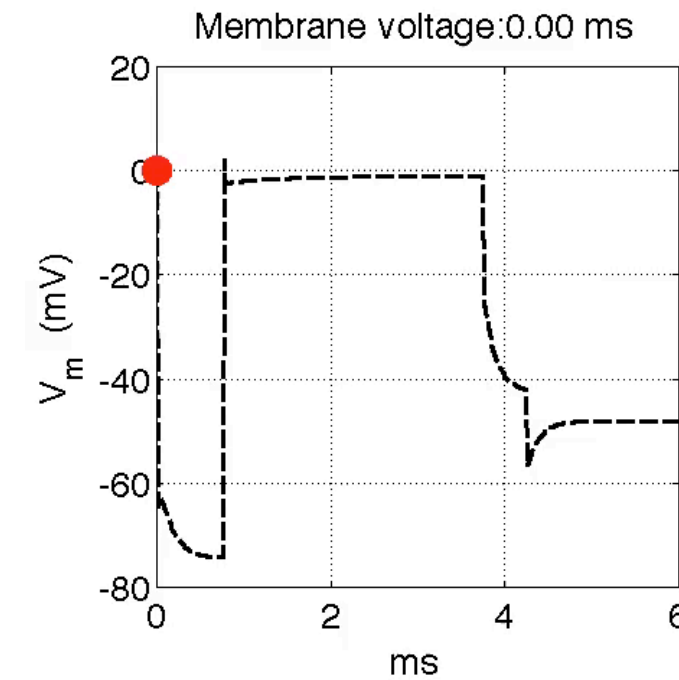
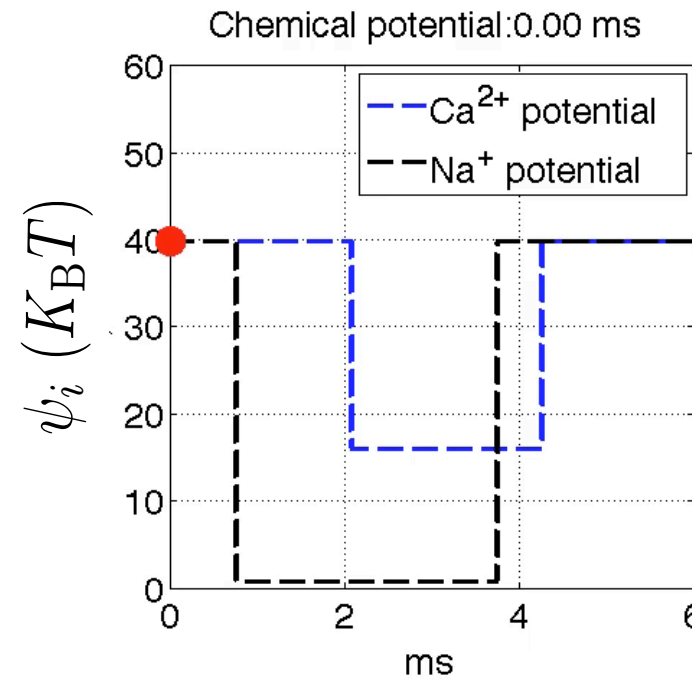
$$P(S(t + dt) = S_j | S(t) = S_i) = r_{i,j} dt$$

Markov chain of calcium ion channel,
Bondarenko et al. 2004

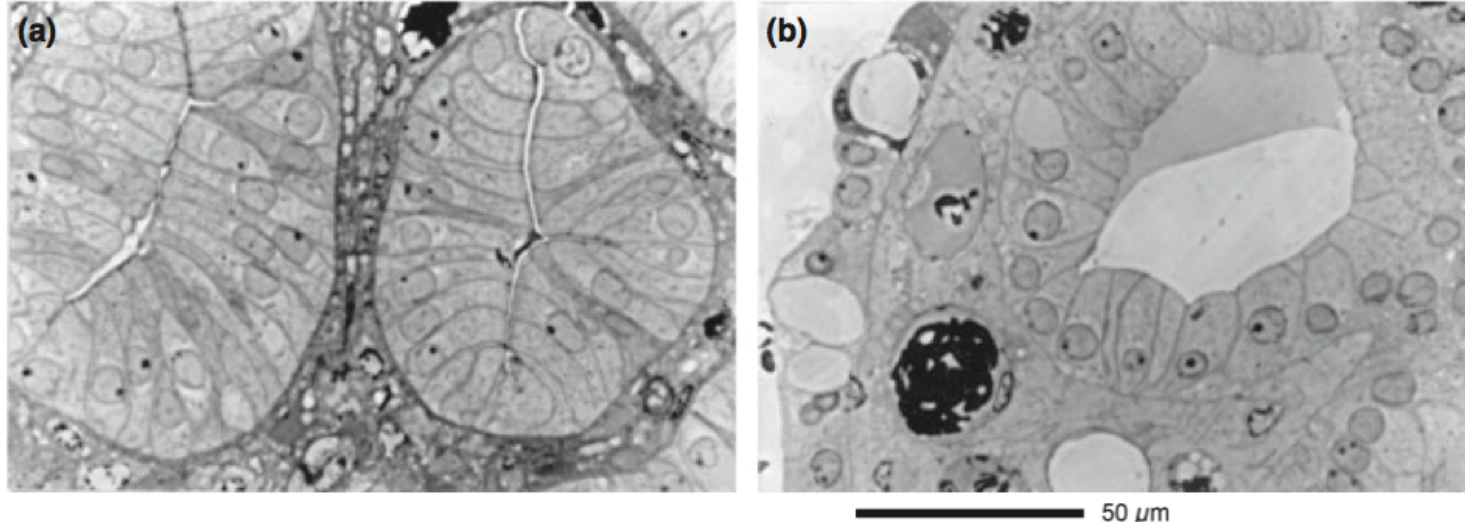


- 4 subunits
- voltage dependent activation
- intracellular calcium and voltage dependent inactivation

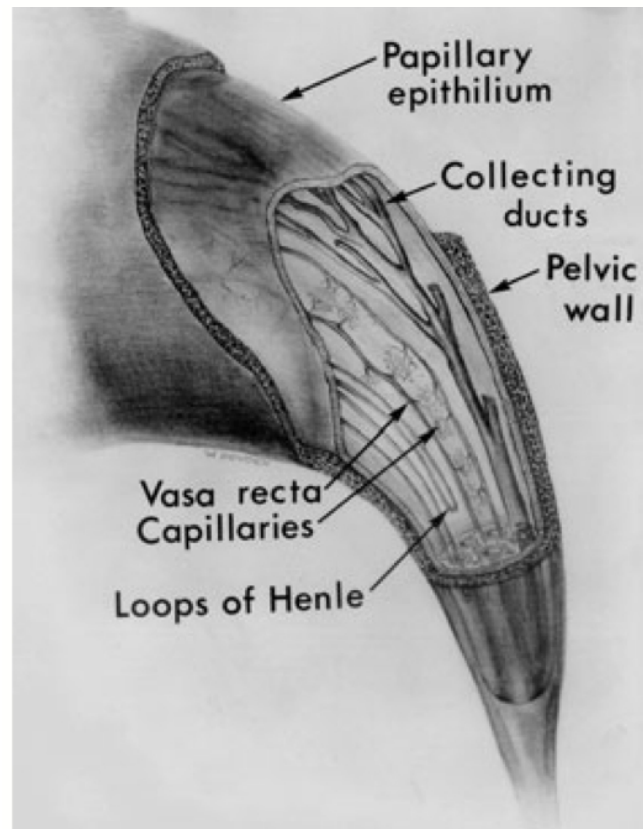
Voltage sensitive calcium ion channels in a dendritic spine



Renal peristaltic concentration



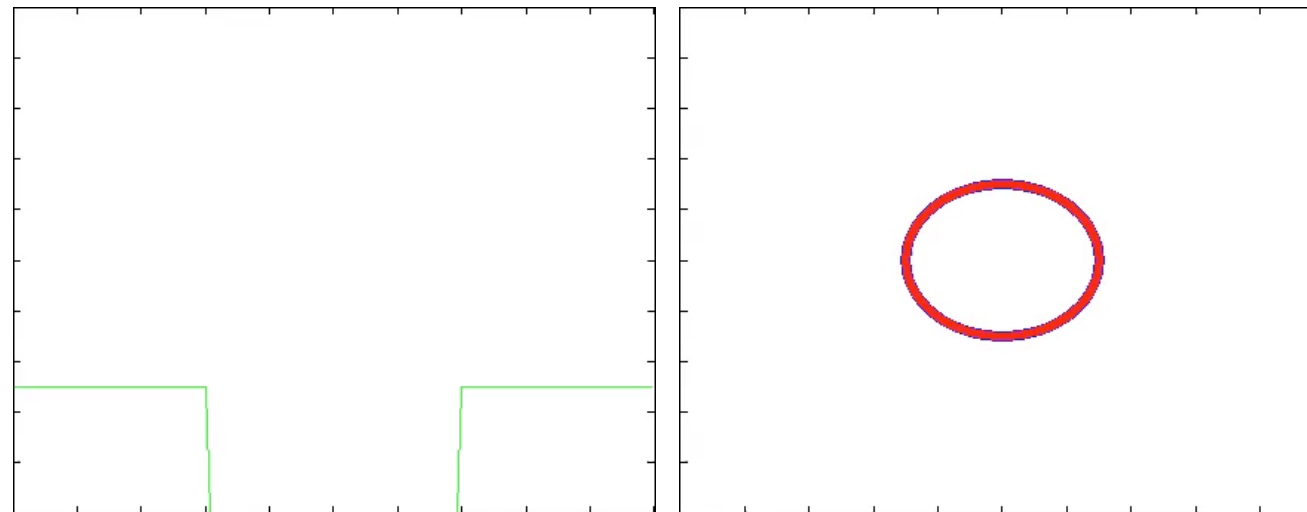
A cross-section of papilla 300 micron above the tip, collecting ducts (a) closed with peristaltic contraction and (b) open with peristaltic relaxation



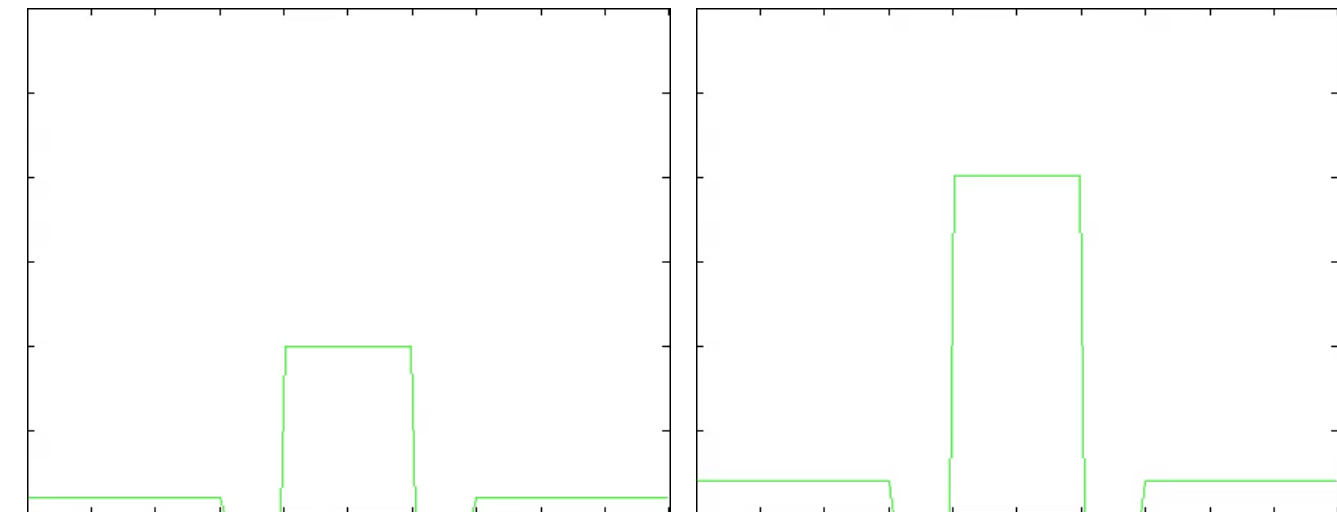
(Lower left) Schematic drawing of a hamster papilla

Osmotic volume change

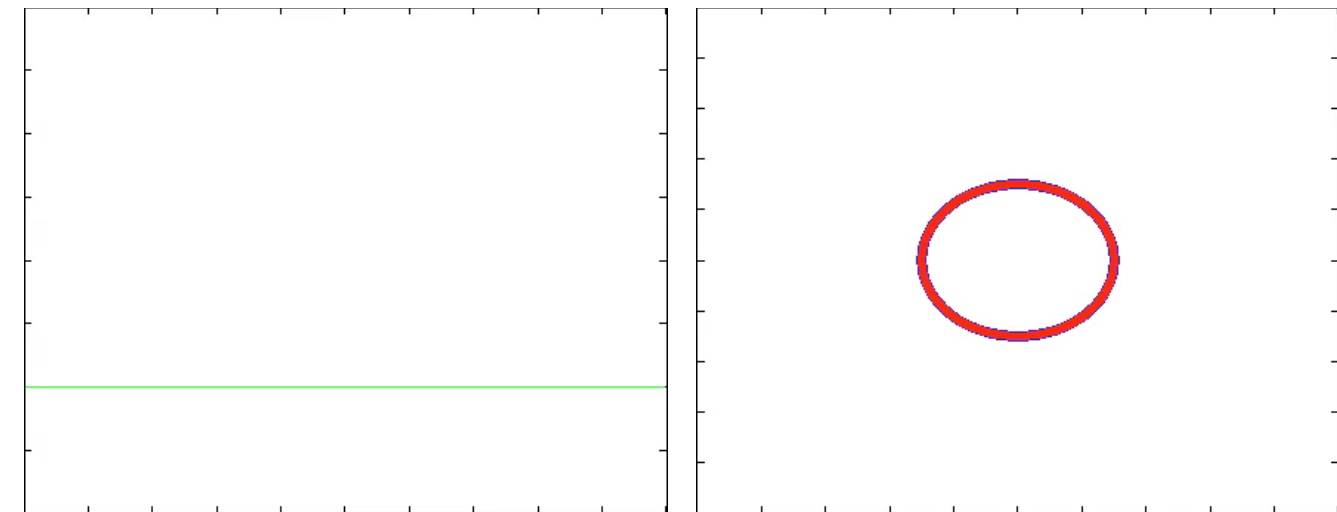
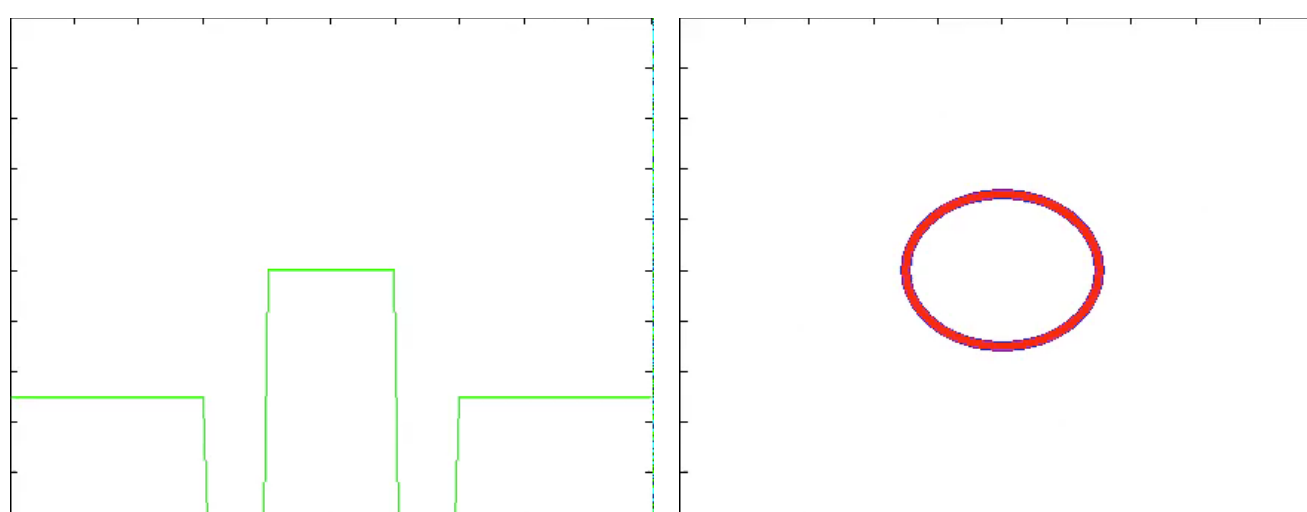
I. Water semi-permeable vesicle with hypotonic distribution



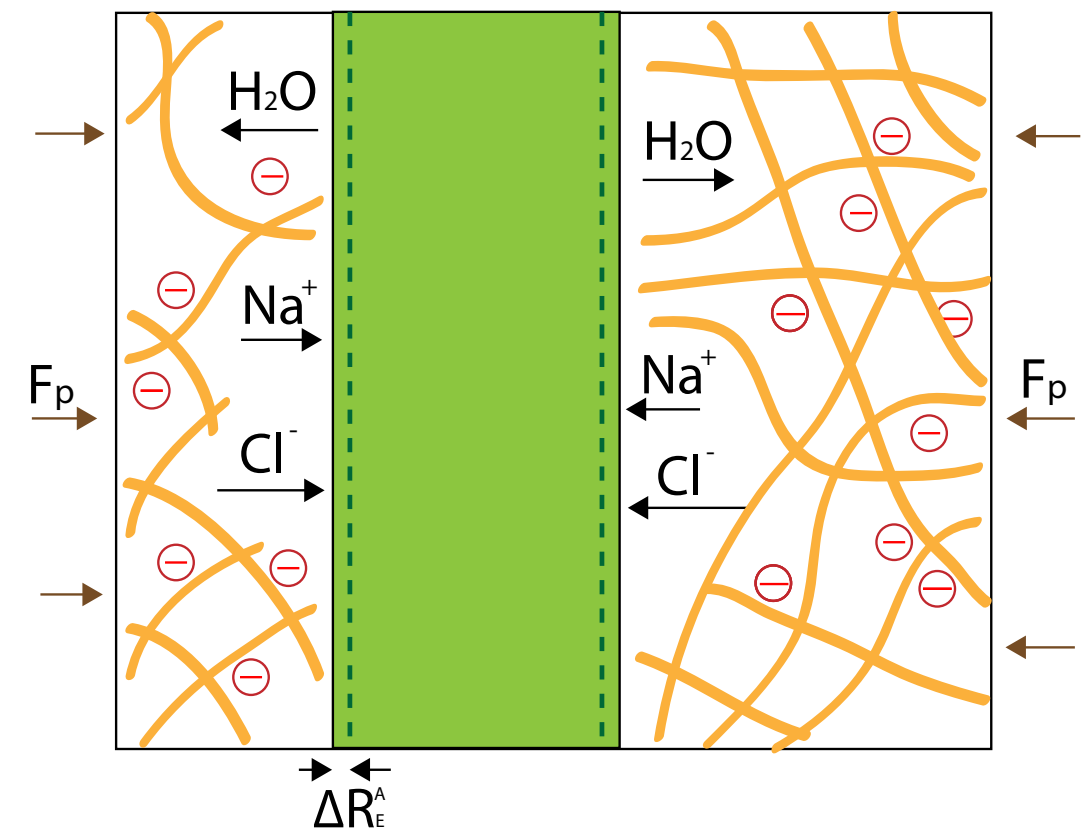
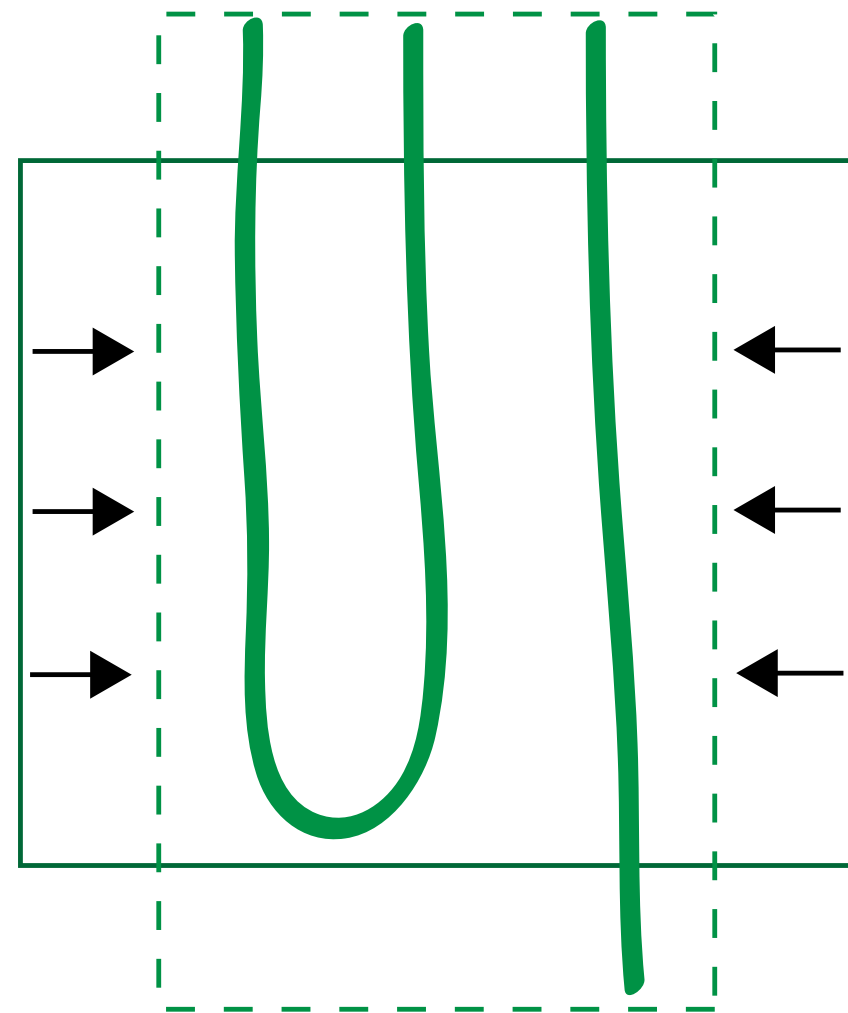
III. Water semi-permeable vesicle with hypertonic distribution



II. Water semi-permeable vesicle in equilibrium

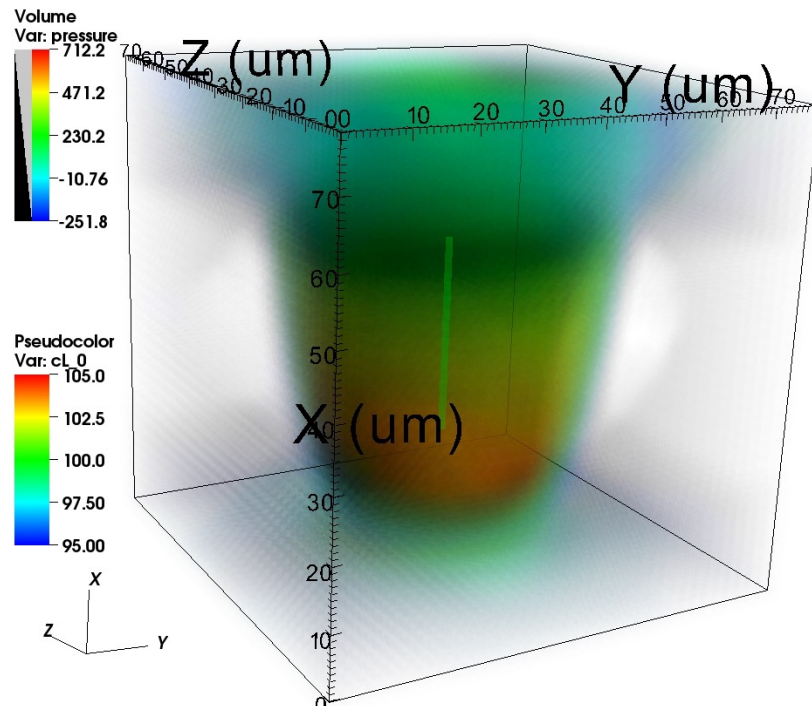


Renal peristaltic concentration

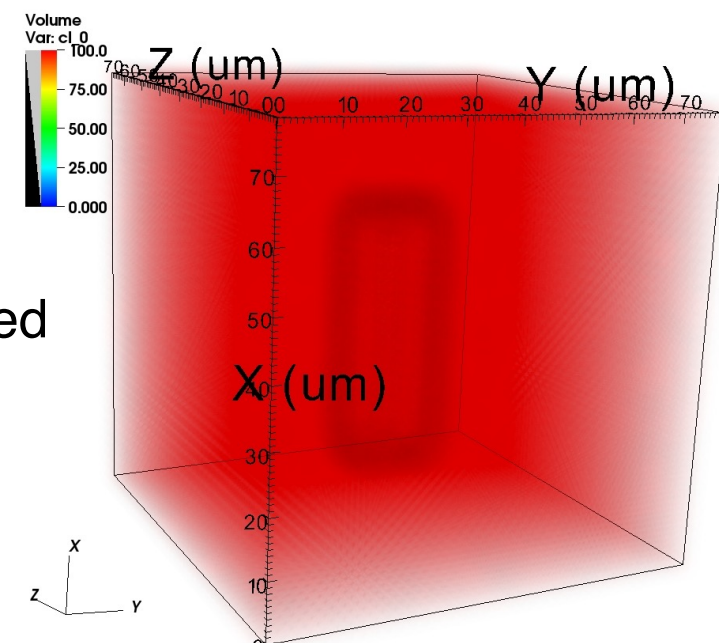


Hypothesized mechanisms of **rectified transport** of ions across epithelial layer via i) **electrically charged** and ii) **viscoelastic extracellular matrix**

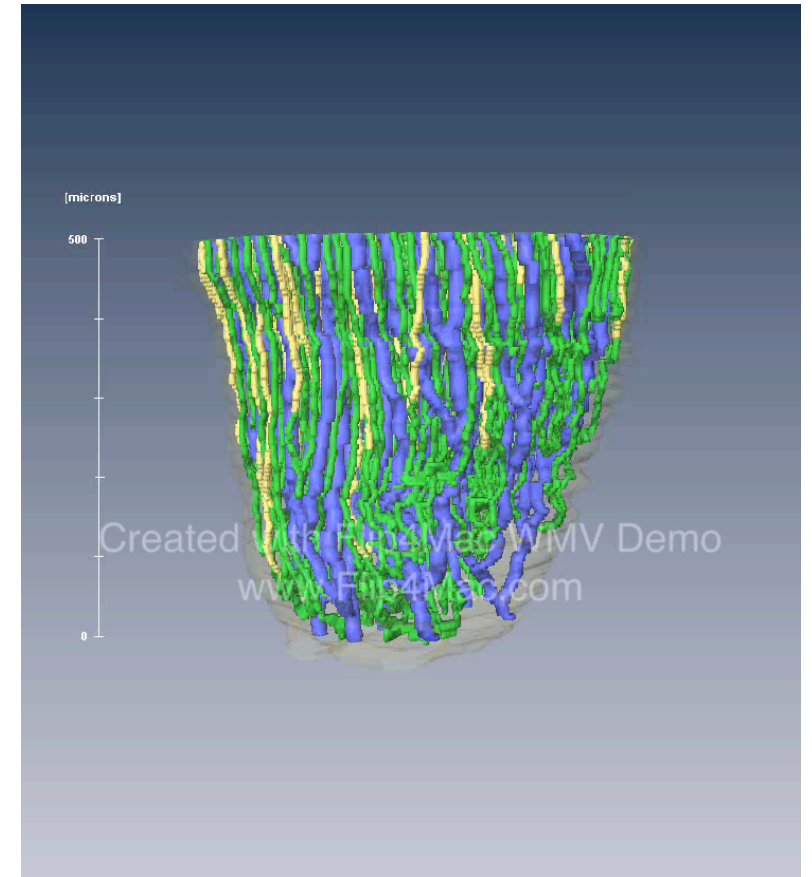
Renal peristaltic concentration



3D hydrostatic pressure distribution from peristaltic contraction and the luminal concentration in collecting duct



3D solute concentration in interstitium using the immersed boundary method with **chemical potential barrier**



3D reconstruction of all papillary collecting ducts (AQP2, blue), ascending thin limbs (CIC-K1, green), and descending thin limbs (AQP1-null, yellow) in a kidney.

T.L. Pannabecker and W.H. Dantzler, 2007

The way to go is to take realistic 1D tubules in 3D, and combine counter-current and peristaltic mechanisms in the renal concentration.

IB method for two-phase fluids and gels

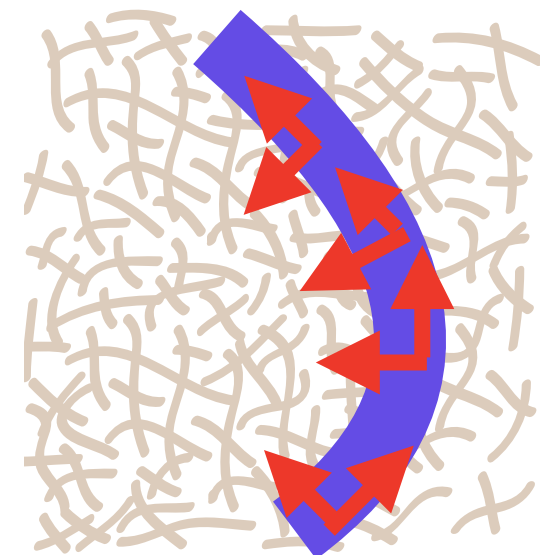
$$\frac{\partial \phi}{\partial t} + \nabla \cdot (\phi \mathbf{v}_p) = 0$$

$$\rho_f \frac{\partial \mathbf{v}_f}{\partial t} + \Gamma(\mathbf{v}_f - \mathbf{v}_p) = -(1 - \phi) \nabla p + \eta_f \nabla \cdot (\nabla \mathbf{v}_f + \nabla \mathbf{v}_f^T) + S \mathbf{F}_f$$

$$\begin{aligned} \rho_p \frac{\partial \mathbf{v}_p}{\partial t} + \Gamma(\mathbf{v}_p - \mathbf{v}_f) &= -\phi \nabla p - \sigma_0 \nabla \phi \\ &\quad + \eta_p \nabla \cdot (\nabla \mathbf{v}_p + \nabla \mathbf{v}_p^T) + \mu \nabla \cdot (\nabla \mathbf{u} + \nabla \mathbf{u}^T) + S \mathbf{F}_p. \end{aligned}$$

$$\frac{d\mathbf{u}}{dt} = \frac{\partial \mathbf{u}}{\partial t} + \mathbf{v}_p \cdot \nabla \mathbf{u} = \mathbf{v}_p$$

$$\nabla \cdot \{(1 - \phi)\mathbf{v}_f + \phi \mathbf{v}_p\} = 0$$



$$\mathbf{F}_p \cdot \mathbf{T} = \Xi_T S^* (\mathbf{v}_f - \mathbf{v}_p) \cdot \mathbf{T}$$

$$\mathbf{F}_p \cdot \mathbf{N} = \Xi_N S^* (\mathbf{v}_f - \mathbf{v}_p) \cdot \mathbf{N}$$

$$\mathbf{F}_f + \mathbf{F}_p = -\frac{\delta E}{\delta \mathbf{X}}$$

IB method for two-phase fluids and gels

Semi-implicit approximate projection approach

STEP I) without volume conservation condition

$$\frac{\phi^{n+\frac{1}{2}} - \phi^n}{\Delta t/2} + D_h \cdot (\phi^n \mathbf{v}_p^n) = 0 \quad \mathcal{L}_h = L_h + G_h D_h \cdot$$

$$\rho_f \frac{\mathbf{v}_f^* - \mathbf{v}_f^n}{\Delta t} + \Gamma(\mathbf{v}_f^{n+\frac{1}{2},*} - \mathbf{v}_p^{n+\frac{1}{2},*}) = -(1 - \phi^{n+\frac{1}{2}}) G_h p^{n-\frac{1}{2}} \\ + \eta_f \mathcal{L}_h \mathbf{v}_f^{n+\frac{1}{2},*} + S_{n+\frac{1}{2}} \mathbf{F}_f^{n+\frac{1}{2},*}$$

$$\rho_p \frac{\mathbf{v}_p^* - \mathbf{v}_p^n}{\Delta t} + \Gamma(\mathbf{v}_p^{n+\frac{1}{2},*} - \mathbf{v}_f^{n+\frac{1}{2},*}) = -\phi^{n+\frac{1}{2}} G_h p^{n-\frac{1}{2}} - \sigma_0 G_h \phi^{n+\frac{1}{2}} \\ + \eta_p \mathcal{L}_h \mathbf{v}_p^{n+\frac{1}{2},*} + \mu \mathcal{L}_h \mathbf{u}^{n+\frac{1}{2}} + S_{n+\frac{1}{2}} \mathbf{F}_p^{n+\frac{1}{2},*}$$

$$\frac{\mathbf{u}^{n+\frac{1}{2}} - \mathbf{u}^n}{\Delta t/2} + \mathbf{v}_p^n \cdot G_h \mathbf{u}^n = \mathbf{v}_p^n$$

$$\mathbf{v}_f^{n+\frac{1}{2},*} = \frac{\mathbf{v}_f^n + \mathbf{v}_f^*}{2}, \quad \mathbf{v}_p^{n+\frac{1}{2},*} = \frac{\mathbf{v}_p^n + \mathbf{v}_p^*}{2}$$

$$\mathbf{F}_p^{n+\frac{1}{2},*} = \Xi_T(\mathbf{v}_f^{n+\frac{1}{2},*} - \mathbf{v}_p^{n+\frac{1}{2},*}) \cdot \mathbf{T}^{n+\frac{1}{2}} \mathbf{T}^{n+\frac{1}{2}}$$

$$+ \Xi_N(\mathbf{v}_f^{n+\frac{1}{2},*} - \mathbf{v}_p^{n+\frac{1}{2},*}) \cdot \mathbf{N}^{n+\frac{1}{2}} \mathbf{N}^{n+\frac{1}{2}}$$

$$\mathbf{F}_f^{n+\frac{1}{2},*} = -\frac{\partial E}{\partial \mathbf{X}^{n+\frac{1}{2}}} - \mathbf{F}_p^{n+\frac{1}{2},*}$$

$$\frac{\mathbf{X}^{n+\frac{1}{2}} - \mathbf{X}^n}{\Delta t/2} = S_n^* \mathbf{v}_f^n$$

IB method for two-phase fluids and gels

Semi-implicit approximate projection approach

STEP II) with approximate projection

$$\frac{\phi^{n+1} - \phi^n}{\Delta t} + D_h \cdot (\phi^{n+\frac{1}{2}} \mathbf{v}_p^{n+\frac{1}{2}}) = 0$$

$$\rho_f \frac{\mathbf{v}_f^{n+1} - \mathbf{v}_f^n}{\Delta t} + \Gamma(\mathbf{v}_f^{n+\frac{1}{2}} - \mathbf{v}_p^{n+\frac{1}{2}}) = -(1 - \phi^{n+\frac{1}{2}}) G_h p^{n+\frac{1}{2}} \\ + \eta_f \mathcal{L}_h \mathbf{v}_f^{n+1} + S_{n+\frac{1}{2}} \mathbf{F}_f^{n+1}$$

$$\rho_p \frac{\mathbf{v}_p^{n+1} - \mathbf{v}_p^n}{\Delta t} + \Gamma(\mathbf{v}_p^{n+\frac{1}{2}} - \mathbf{v}_f^{n+\frac{1}{2}}) = -\phi^{n+\frac{1}{2}} G_h p^{n+\frac{1}{2}} - \sigma_0 G_h \phi^{n+\frac{1}{2}} \\ + \eta_p \mathcal{L}_h \mathbf{v}_p^{n+1} + \mu \mathcal{L}_h \mathbf{u}^{n+\frac{1}{2}} + S_{n+\frac{1}{2}} \mathbf{F}_p^{n+1}$$

$$\mathbf{F}_p^{n+1} = \Xi_T (\mathbf{v}_f^{n+1} - \mathbf{v}_p^{n+1}) \cdot \mathbf{T}^{n+\frac{1}{2}} \mathbf{T}^{n+\frac{1}{2}} \\ + \Xi_N (\mathbf{v}_f^{n+1} - \mathbf{v}_p^{n+1}) \cdot \mathbf{N}^{n+\frac{1}{2}} \mathbf{N}^{n+\frac{1}{2}}$$

$$\mathbf{F}_f^{n+1} = -\frac{\partial E}{\partial \mathbf{X}^{n+\frac{1}{2}}} - \mathbf{F}_p^{n+1}$$

$$(1 - \phi^{n+1}) \mathbf{v}_f^{n+1} + \phi^{n+1} \mathbf{v}_p^{n+1} = \\ (I - G_h L_h^{-1} D_h) (1 - \phi^{n+1}) \mathbf{v}_f^* + \phi^{n+1} \mathbf{v}_p^*$$

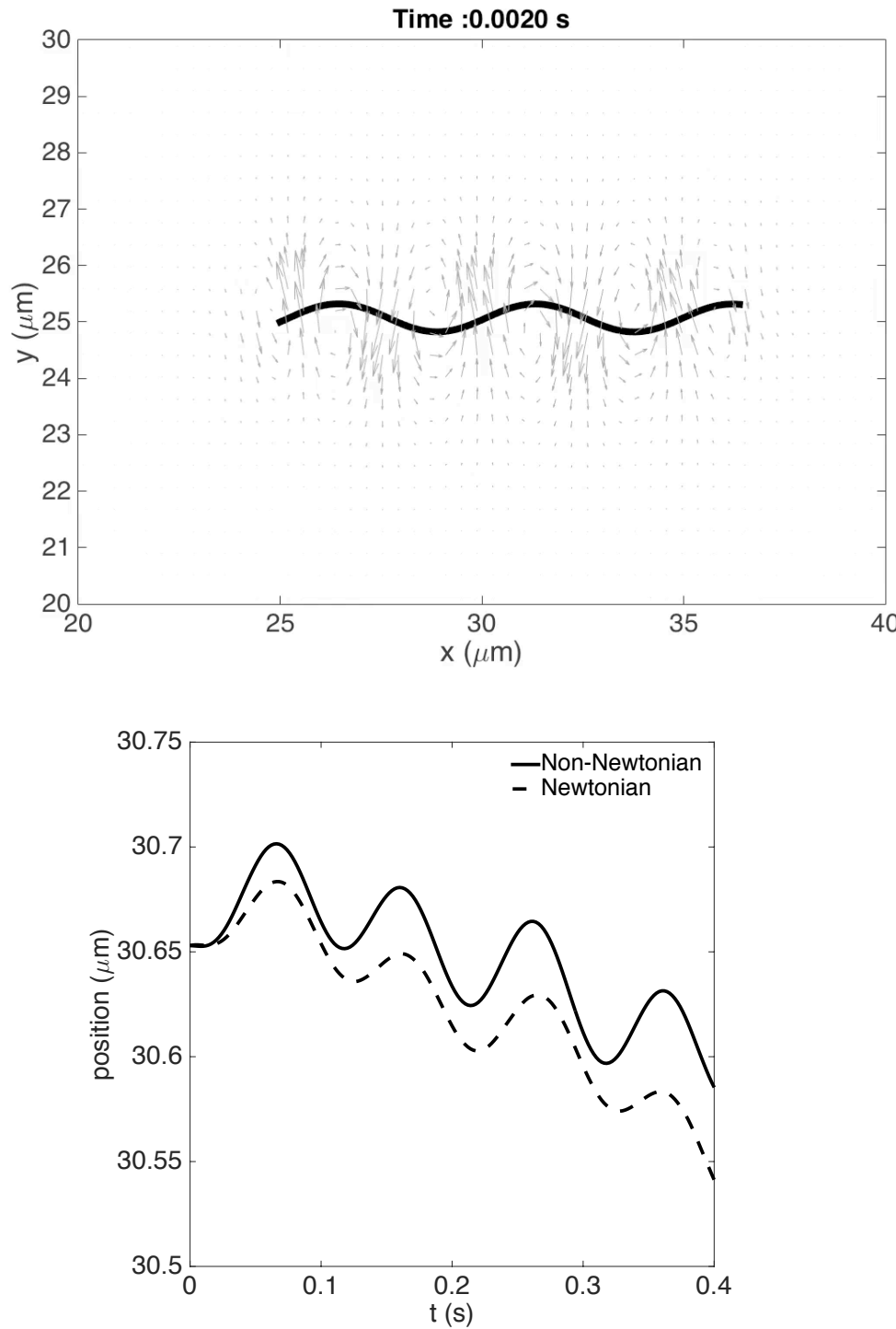
$$\frac{\mathbf{u}^{n+1} - \mathbf{u}^n}{\Delta t} + \mathbf{v}_p^{n+\frac{1}{2}} \cdot G_h \mathbf{u}^{n+\frac{1}{2}} = \mathbf{v}_p^{n+\frac{1}{2}}$$

$$\frac{\mathbf{X}^{n+1} - \mathbf{X}^n}{\Delta t} = S_n^* \mathbf{v}_f^{n+\frac{1}{2}}$$

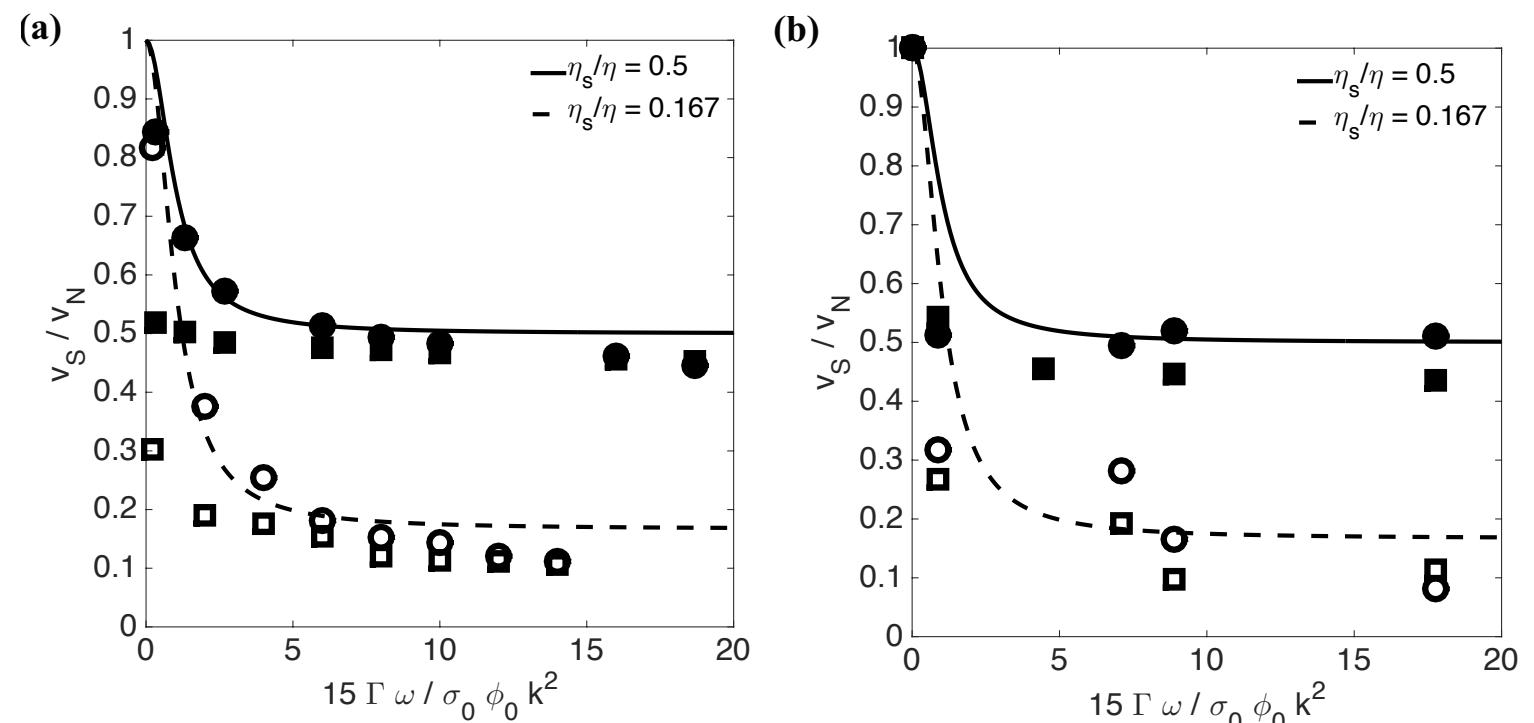
$$p^{n+\frac{1}{2}} - p^{n-\frac{1}{2}} = L_h^{-1} D_h \cdot \left\{ \rho_f \frac{\mathbf{v}_f^* - \mathbf{v}_f^{n+1}}{\Delta t} + \rho_p \frac{\mathbf{v}_p^* - \mathbf{v}_p^{n+1}}{\Delta t} \right. \\ \left. + \eta_f \mathcal{L}_h (\mathbf{v}_f^{n+1} - \mathbf{v}_f^{n+\frac{1}{2},*}) + \eta_p \mathcal{L}_h (\mathbf{v}_p^{n+1} - \mathbf{v}_p^{n+\frac{1}{2},*}) \right\}$$

IB method for two-phase fluids and gels

Two phase vs. single phase / Oldroyd B



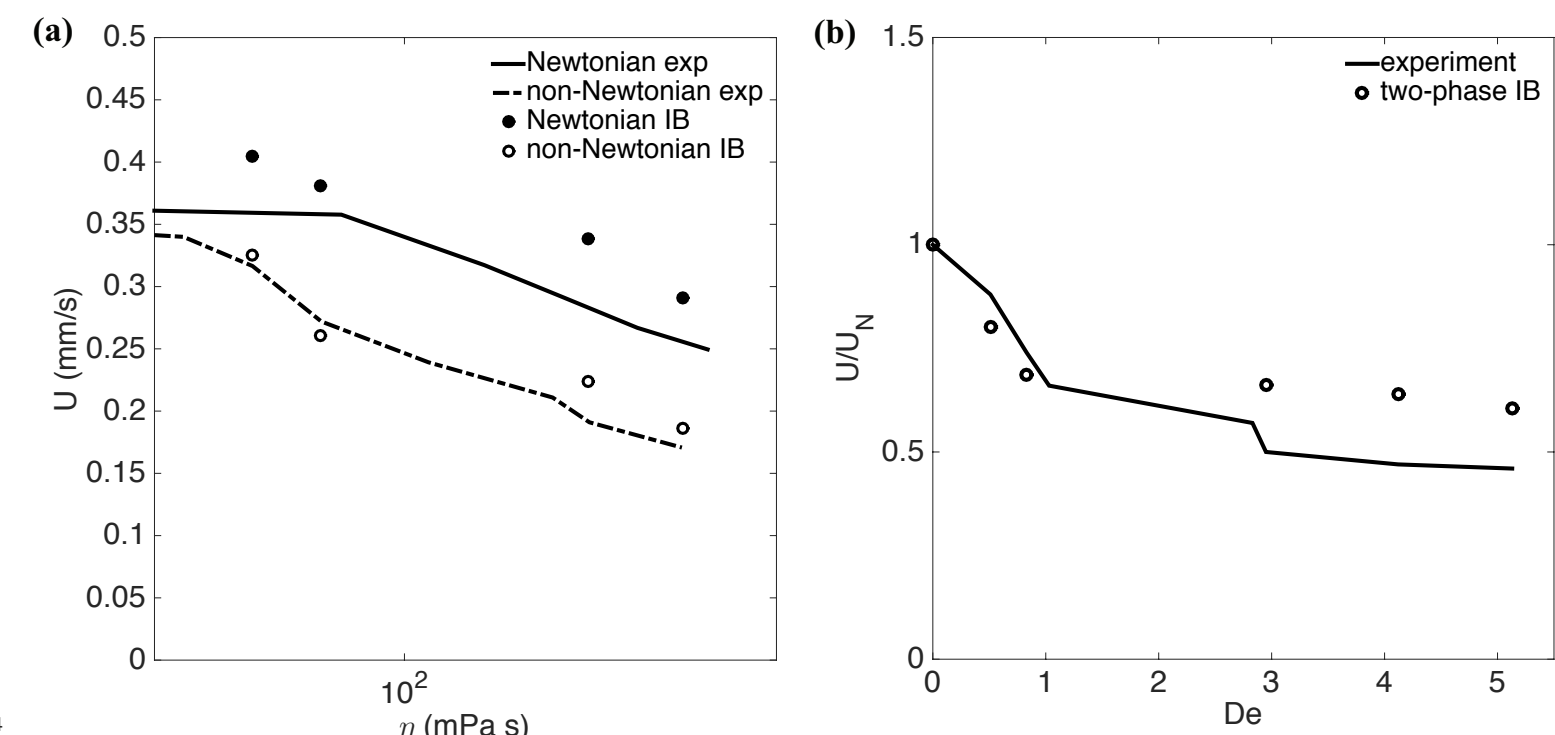
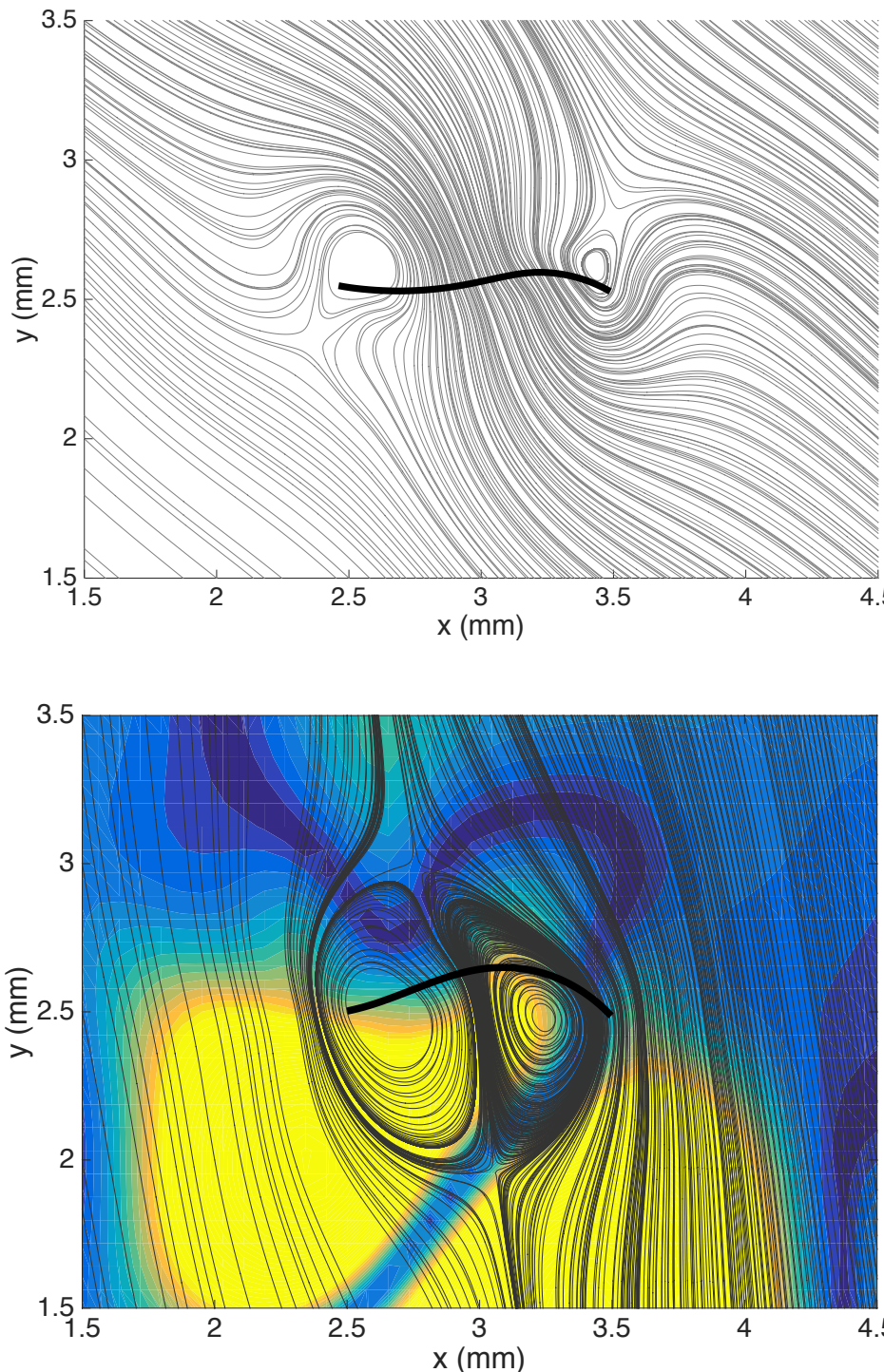
$$V_S/V_N = \frac{1 + \eta_S/\eta \text{ } De^2}{1 + De^2} \quad \text{Lauga, 2007}$$



(a) small amplitude, infinite
(b) finite length swimmer

IB method for two-phase fluids and gels

C. elegans swimming / hyperbolic extensional flows



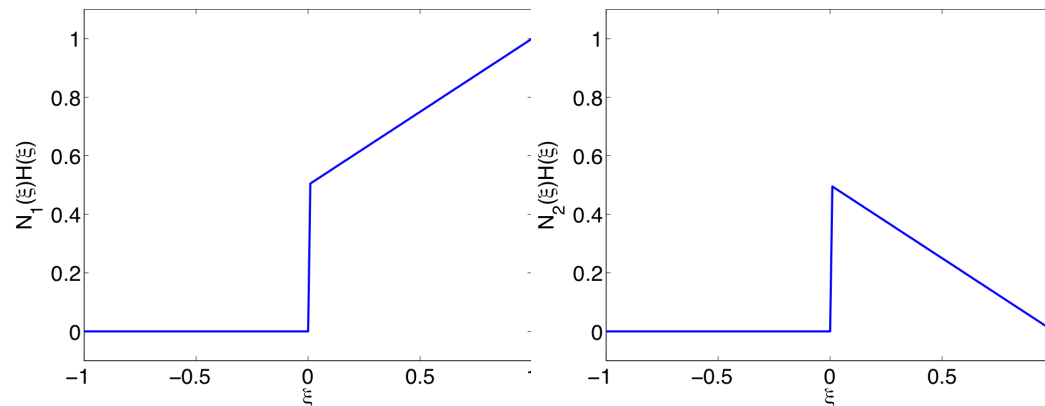
Experiments: Arratia lab

Flow streamlines about a swimming *C. elegans*. The colormap shows the magnitude of the trace of the elastic stress.

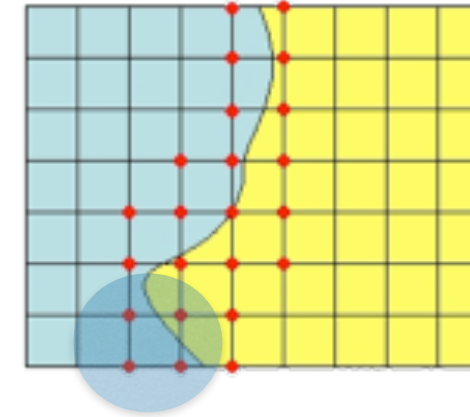
Future work

IB for advection-electrodiffusion with DG/XFEM

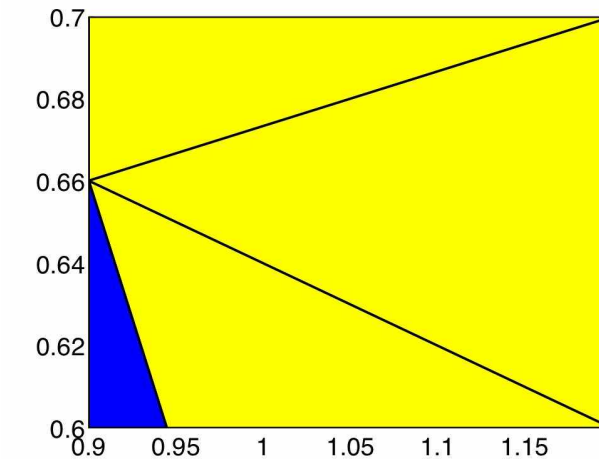
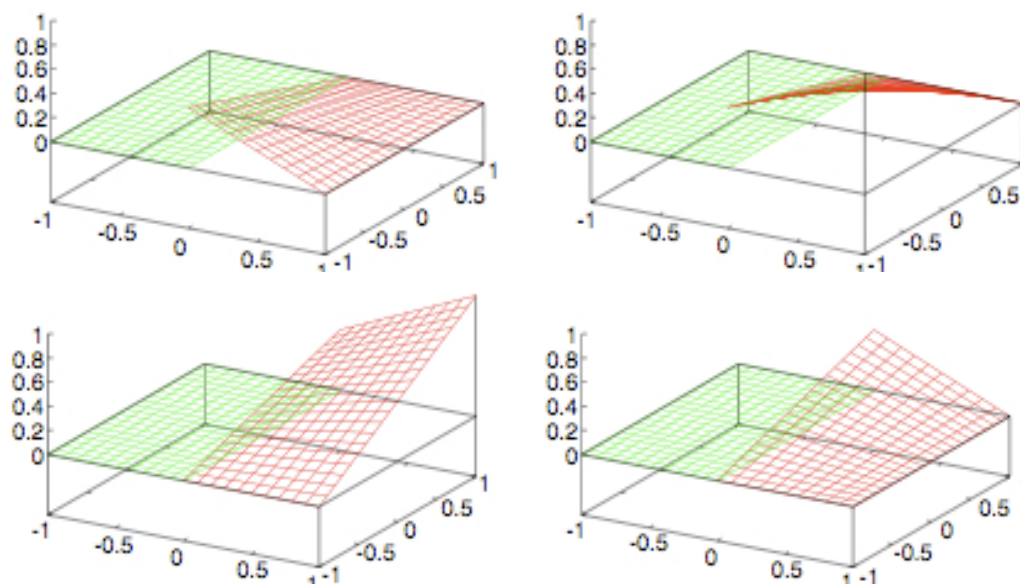
extended shape function 1D



enriched nodes



extended shape function 2D



Integration by Delaunay triangulation

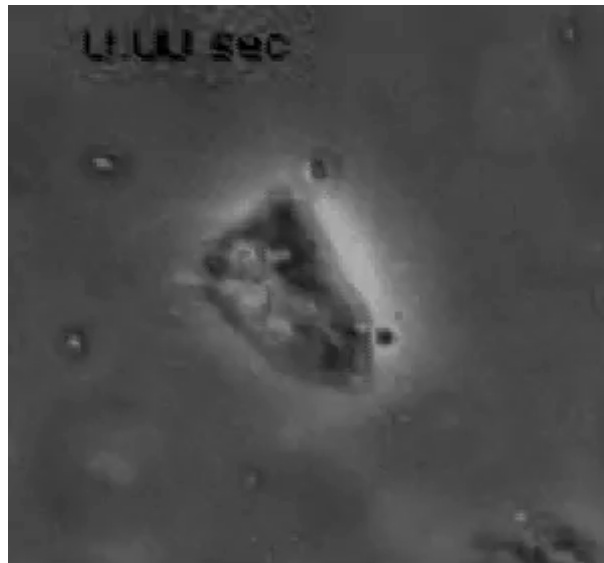
IB for two-phase viscoelastic fluids

Fast composite multigrid as preconditioner

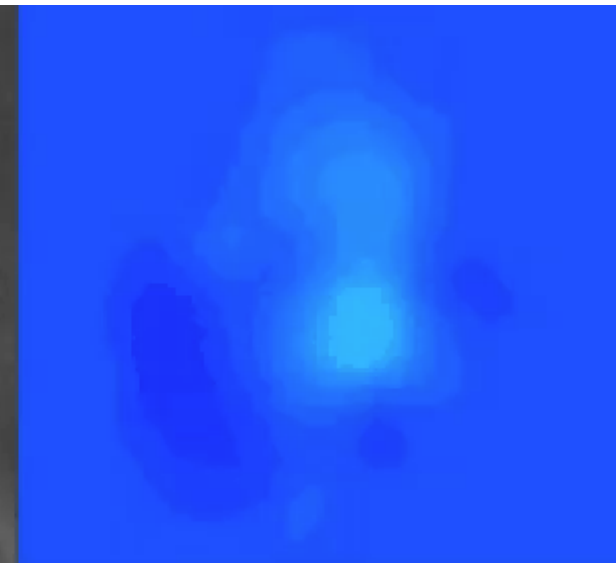
Exact projection method, MAC scheme

Mechano-sensing of cardiac differentiation

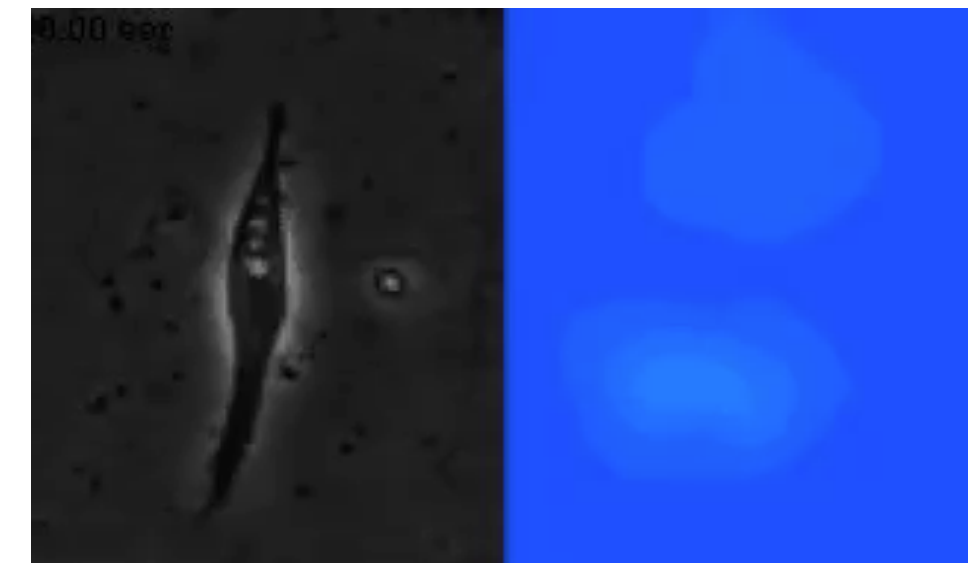
Embryonic cardiac myocytes contraction vs. microenvironment



Engler, et al. 2008



soft gel strain



stiff gel strain

How the following developmental mechanisms are influenced by mechanical microenvioronment?

- myofibrillogenesis
- biogenesis
- calcium handling
- mitochondria PTP gating and volume regulation

Acknowledgement

Charles Peskin, Courant Institute, New York University

Boyce Griffith, University of North Carolina

Charles Wolgemuth, University of Arizona

Daniel Beard, University of Michigan

Eric Sobie, Mount Sinai School of Medicine

Paul Arratia, University of Pennsylvania

NIH P50 GM094503

NIH R01 GM072004